GEODYNAMICS & TECTONOPHYSICS
Published by the Institute of the Earth's Crust, Siberian Branch, Russian Academy of Sciences

PALEOGEODYNAMICS

2022 VOLUME 13 ISSUE 3 ARTICLE 0636

ISSN 2078-502X

DOI: 10.5800/GT-2022-13-3-0636

GEOCHEMICAL MARKERS OF THE JOINT STRUCTURAL AND COMPOSITIONAL EVOLUTION OF THE BASEMENT AND COVER (NORTHERN LADOGA SWECOFENNIDES, RUSSIA)

Yu.A. Morozov [1], **E.N. Terekhov** [2], **M.A. Matveev** [1]✉, **O.I. Okina** [2]

[1] Schmidt Institute of Physics of the Earth, Russian Academy of Sciences, 10-1 Bolshaya Gruzinskaya St, Moscow 123242, Russia

[2] Geological Institute, Russian Academy of Sciences, 7-1 Pyzhevsky Ln, Moscow 119017, Russia

ABSTRACT. Detailed studies of the deeply metamorphosed Early Precambrian rocks of the Northern Ladoga region allowed us to distinguish three deformation stages of the Svecofennian tectogenesis during which there occurred significant structural and compositional transformations of the "cover (Paleoproterozoic) – basement (Archean)" system. In addition to the structural-paragenetic analysis, which allowed to allocate transversal structural paragenesis in both floors, there are some other opportunities in the recognition of their-hosted granitoid veined bodies with a positive Eu anomaly. The rock varieties with this anomaly are always high in barium and do not show a direct correlation between the Eu anomaly and $(La/Yb)_n$, Ca and Sr. This is contrary to the ideas about the occurrence of a positive Eu anomaly due to the substitution of divalent strontium by Eu^{++} and suggests that the formation of such rocks took place under the influence of deep reduced fluids. It was found that granitoids with a positive Eu anomaly were formed during the first and last stages of the structure evolution, with a predominance of brittle deformations and a deep-reduced fluid breakthrough. At the second stage, with the dominant manifestation of plastic deformations, when such fluids could be "blocked" within the system, there was a formation of granitoids with low barium concentrations and a negative Eu anomaly.

KEYWORDS: Northern Ladoga region; tectonic deformations; metamorphism; geochemistry; Svecofennian tectogenesis; granitoids; Eu anomaly; platform evolution

FUNDING: The study was carried out under the state assignments of the Schmidt Institute of Physics of the Earth, Russian Academy of Sciences, (for matters relating to the interaction of endogenous processes during the formation of the continental crust), in accordance with the plans for fundamental research of the Geological Institute Russian Academy of Sciences and with a financial support by the Russian Foundation for Basic Research under grant 19-05-00256 (for matters relating to synmetamorphic formation of structures in the "basement – cover" system).

RESEARCH ARTICLE

Received: May 25, 2021
Revised: October 10, 2021
Accepted: October 11, 2021

Correspondence: Maksim A. Matveev, matveevmaksim93@mail.ru

FOR CITATION: Morozov Yu.A., Terekhov E.N., Matveev M.A., Okina O.I., 2022. Geochemical Markers of the Joint Structural and Compositional Evolution of the Basement and Cover (Northern Ladoga Swecofennides, Russia). Geodynamics & Tectonophysics 13 (3), 0636. doi:10.5800/GT-2022-13-3-0636

ГЕОХИМИЧЕСКИЕ МЕТКИ СОВМЕСТНОЙ СТРУКТУРНО-ВЕЩЕСТВЕННОЙ ЭВОЛЮЦИИ ЧЕХЛА И ФУНДАМЕНТА (СВЕКОФЕННИДЫ СЕВЕРНОГО ПРИЛАДОЖЬЯ, РОССИЯ)

Ю.А. Морозов[1], Е.Н. Терехов[2], М.А. Матвеев[1], О.И. Окина[2]

[1] Институт физики Земли им. О.Ю. Шмидта РАН, 123242, Москва, ул. Большая Грузинская, 10, стр. 1, Россия
[2] Геологический институт РАН, 119017, Москва, Пыжевский пер., 7, стр. 1, Россия

АННОТАЦИЯ. Детальные исследования глубокометаморфизованных раннедокембрийских пород Северного Приладожья позволили выделить три этапа деформаций эпохи свекофеннского тектогенеза, в ходе которых произошли существенные структурно-вещественные преобразования системы «чехол (палеопротерозой) – фундамент (архей)». Помимо проведенного структурно-парагенетического анализа, позволившего выделять «сквозные» структурные парагенезы в обоих этажах, дополнительные возможности открываются при выделении вписанных в них гранитоидных жильных образований с выявленной положительной Eu-аномалией. Разности, имеющие эту аномалию, всегда обогащены барием и не показывают прямую корреляцию величины Eu-аномалии с $(La/Yb)_n$, Ca и Sr. Это противоречит представлениям о причинах появления положительной Eu-аномалии за счет замещения двухвалентного стронция Eu^{++} и позволяет предположить, что формирование подобных пород происходило под влиянием глубинных восстановленных флюидов. Установлено, что гранитоиды с положительной Eu-аномалией формировались на первом и заключительном этапах эволюции структуры, когда преобладали хрупкие деформации и происходил прорыв глубинных восстановленных флюидов. На втором этапе, с доминирующим проявлением пластических деформаций, когда могла происходить «закупорка» таких флюидов внутри системы, формировались гранитоиды с низкими концентрациями бария и отрицательной Eu-аномалией.

КЛЮЧЕВЫЕ СЛОВА: Северное Приладожье; тектонические деформации; метаморфизм; геохимия; гранитоиды; свекофеннский тектогенез; Eu-аномалия; эволюция платформы

ФИНАНСИРОВАНИЕ: Работа выполнена в рамках исследований по государственному заданию ИФЗ РАН (в части вопросов взаимодействия эндогенных процессов при формировании континентальной земной коры), в соответствии с планами фундаментальных исследований ГИН РАН и по гранту РФФИ № 19-05-00256 (в части аспектов метаморфогенного структурообразования в системе «чехол – фундамент»).

1. INTRODUCTION

The problems of deformational-metamorphic evolution of the crystalline basement complexes and overlying sediment become a matter of considerable importance in the study of structural features and a polystage development of ancient mobile belts [Watson, Dunning, 1979; Park, Bowes, 1983; Bowes et al., 1984; Morozov, Somin, 1997; Morozov et al., 2000]. This particularly applies to deep tectonothermal reworking of the "basement – cover" system and accompanied phenomena of intensive rheomorphism of the basement and its structural and compositional and rheological similarities with the overlying metamorphosed supracrustal units when their separation and determination of the interface between them become difficult [Morozov et al., 2020]. Of similar independence and importance is the task of distinguishing the structural elements and superimposed mineral formations in the basement complexes occurred as a result of tectogenetic events typical for the "basement – cover" system. Besides the structural analysis, making it possible to distinguish transversal structural parageneses in both floors, there will be other opportunities to identify structural and compositional makers (dykes, veins, localized deformation zones) of compatible tectonothermal events for which there is an opportunity to determine depths (by mineral-phase thermobarometric methods), time limits and their formation intervals (isotope dating) and to identify general geochemical markers for correlation between coeval structural elements in the cover and basement in the form of similar, contrast or anomalous behavior of main and minor – including rare earth (REE) – elements. Of particular importance is the study of causes which give rise to the Eu anomaly in pegmatite veins – a sort of markers of deformation stages and extension structures.

The largest negative Eu anomalies that probably determine the intermediate upper crust occur in granites and metasomatites for which Eu/Eu* is sometimes less than 0.01 [Kostitsyn, 2000], i.e., Eu concentrations are 100 times less than they should have been judging on other REE distributions. A widespread occurrence of the rocks with negative Eu anomalies in the post-Archean formations and, consequently, the existence of typical REE distribution in the post-Archean sediments (PAAS curve showing the intermediate eroded units) implies the existence of deep-seated (lower-mid-crustal) rocks with a complementary character of the REE distribution (with a positive Eu anomaly). The identification of reservoir with high Eu concentrations is the subject of a large number of studies [Taylor, McLennan, 1988; Rudnick, 1992]. The most logical would be the situation when basic anhydrous granulites exhausted by lithophylic elements are regarded as restites resulting from the melting of granite cover of the Earth. However, it turned out to be that most of the rocks in the granulite complexes, which are exposed at the surface now and might have been comprised the lower crust before, rarely show the presence of Eu anomalies. Besides, positive Eu anomalies are more typical of acid granulites [Rudnick, 1992], which could not be restites resulting from the upper crust melting. Unlike basic granulites in the area, the granulite xenolithes in volcanic rocks and pipes are almost always characterized by positive Eu anomalies. The same is observed for the eclogite-like rocks uplifted in the form of individual blocks at the root of the rift systems [Terekhov et al., 2016]. Consistent positive Eu anomalies are typical for anorthosites which occupy small volumes in granulite complexes and in vein formations of the final stage of exhumation of these complexes [Terekhov, Shcherbakova, 2006]. Other crustal complexes with a positive Eu anomaly are oil, some coals and partly phosphorites, i.e. the rocks occurred in reducing environments [Baturin et al., 2001]. However, all these formations generally do not have an effect on negative europium balance in the crust due to their small volumes. Note that the rocks with a positive Eu anomaly are more common in the Early Precambrian complexes and less common in geologically recent formations. The occurrence of a positive Eu anomaly is now often attributed to extraordinary character and concentration of fluids accompanying the rock formation processes [Lukanin, Drenov-Pegarev, 2009; Joosua et al., 2016]. Therefore, the study of granite veins with a positive Eu anomaly, not typical of the crustal rocks, will make it possible to understand the specifics of extraordinary petrogenetic conditions which may provide interpretation of the character, geodynamic setting and formation conditions of the Svecokarelides in the Northern Ladoga region. It is from this perspective that we try to identify and to analyze general geochemical features of certain veined bodies and the host substrate in the Archean basement and on the Paleoproterozoic cover, both of which experienced polystage Svecofennian tectogenetic events in the southeastern Baltic (Fennoscandian) Shield (Northern Ladoga region).

2. A GEOLOGICAL OVERVIEW OF THE STUDY AREA

The Northern Ladoga region covers the southeastern part of the Baltic (Fennoscandian) Shield in the conjunction zone between its two large components – Archean Karelian Craton and Paleoproterozoic Svecofennian accretionary orogen [Morozov, Gaft, 1985; Baltybaev et al., 2000; Sharov, 2020]. This area is a part of the Svecokarelian mobile area stabilized in the late Early Proterozoic and structurally and tectonically related to the Savo-Ladoga zone [Salop, 1979] or, in other terms, to the Raahe-Ladoga suture zone [Bowes et al., 1984; Park et al., 1984; Nironen, 1997]. Presented here (Fig. 1, a) is the contemporary erosional truncation of formations of two structural floors of the Baltic Shield – lower (Archean granite-gneisses) and middle (Paleoproterozoic volcano-terrigenous Ladoga complex). The Ladoga complex, partially formed on the Archean crystalline basement of the pericratonic margin of the Karelian massif in the interval from 2.1 to 1.8 Ga, includes the Late Jatulian-Livvian metamorphosed volcanogenic-sedimentary formations, united into the Sortavala Group (2.06–1.98 Ga), and the Kalevian flyschoid-terrigenous sediments comprising the mere Ladoga zone of Karelides (1.97–1.89 Ga). Coeval with the latter, the Svecofennian deposits supposedly constitute the individual Lahdenpoh series, laterally adjacent to the Ladoga series and, according to some researchers [Baltybaev et al., 2000], initiated on the oceanic crust. The formation and evolution of the Ladoga complex in the zone of interaction between two plates – Karelian Craton and Svecofennian oceanic juvenile crust, subducting beneath the Archean craton, allow determining the type of geodynamical setting of that time as a combined subduction-accretionary [Bowes et al., 1984].

The Northern Ladoga region is also a classical area with manifestation of moderate-pressure zonal metamorphism [Velikoslavinsky, 1972; Nagaitsev, 1974]. The degree of metamorphism increases therein from northeast to southwest, from the lower greenschist facies in the narrow stripe adjacent to the Karelian Craton to the granulite facies rocks that commonly occur within the Svecofennian rocks of the Lahdenpoh series (Fig. 1, c). The boundary between the Karelides (northern domain) and the Svecofennides (southern domain) is the so called Meyeri zone [Shuldiner et al., 1995; Baltybaev et al., 1996] (Fig. 1, b, c) composed of tectonic covers of the rocks of the Ladoga and Sortavala series sloping gently southward, with participation of foliated rock bodies of the early kinematic tonalite-trondhjemite-granodiorite (TTG) complex and the Archean granite-gneiss basement layers [Sharov, 2020].

A complex, polystage structural evolution of the region, related primarily to the Svecofennian tectogenetic events (1.89–1.75 Ga) and partly to the subsequent orogenic movements, has at least three main stages (D1, D2, D3) [Morozov et al., 2020] that were distinguished due to kinematic variability in the environment of long-term development of alternating transpression responsible for the formation of the regional flower – inspired divergent structure (Fig. 1, c)

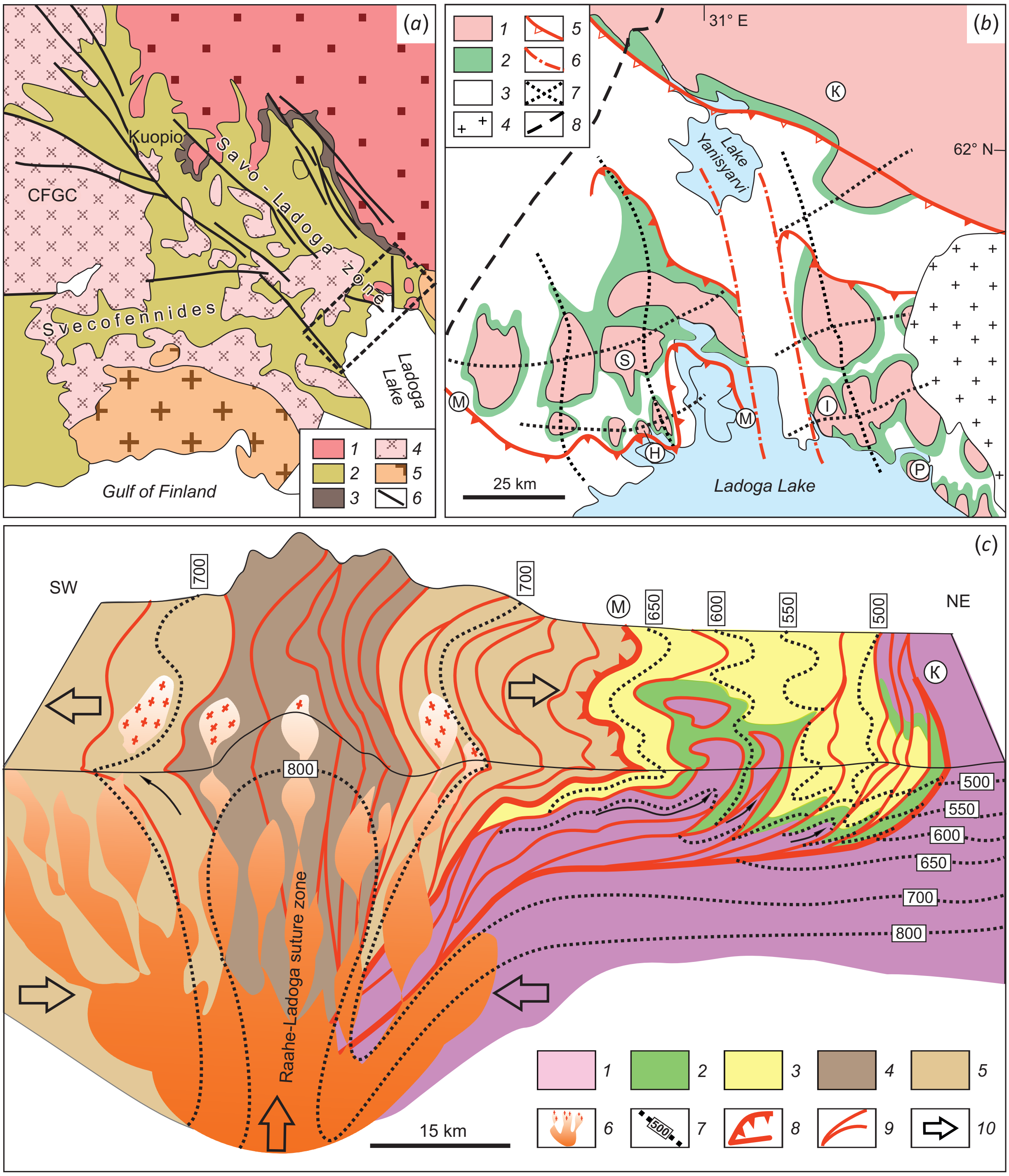

Fig. 1. Structural sketches of the southeastern part of the Baltic Shield.

(*a*) – simplified geological scheme of the Svecofennian complexes on the pericraton margin of the Karelian massif: *1* – Archaean, *2* – Paleoproterozoic (Karelides and Svecofennides), *3* – Jatulian-Livvian complex, *4* – Paleoproterozoic granitoids, *5* – rapakivi granites, *6* – largest faults. CFGC – Central Finland Granitoid Complex. The rectangle marks the research area in the Ladoga region. (*b*) – structure of the northern domain of the Ladoga region: *1* – granite-gneisses of the Archean basement, *2*–*3* – complexes of the Paleoproterozoic cover: *2* – metavolcanics of the Sortavala series, *3* – metapsammites of the Ladoga series, *4* – Mesoproterozoic rapakivi-granites of the Salminsky massif, *5* – the first stage faults, *6* – the second stage faults, *7* – trends of the interference folding systems, *8* – state border. Letters in circles indicate: K – Karelian massif, M – Meyeri zone; dome-shaped basement protrusions: H – Havus, I – Impilahti, P – Putsaari, S – Sortavala. (*c*) – conceptual block-diagram of the Ladoga region tectonic structure: *1* – Archean granite-gneisses, *2* – metavolcanics of the Sortavala series, *3*–*5* – metapsammites of the Ladoga complex in different metamorphic facies, *6* – intrusive formations of the Svecofennian tectogenesis, *7* – metamorphic isogrades, *8* – tectonic sutures, *9* – faults, *10* – tectonic transport directions.

Рис. 1. Обзорные схемы строения юго-восточной части Балтийского щита.

(*а*) – упрощенная геологическая схема расположения комплексов свекофеннид на перикратонной окраине Карельского массива: *1* – архей, *2* – палеопротерозой (карелиды и свекофенниды), *3* – комплекс ятулия – ливвия, *4* – гранитоиды палеопротерозойского возраста, *5* – граниты рапакиви, *6* – крупнейшие разломы. CFGC – Центрально-Финский массив. Прямоугольником выделен район исследований в Приладожье. (*b*) – схема строения северного домена Приладожья: *1* – гранитогнейсы архейского фундамента, *2–3* – комплексы палеопротерозойского чехла: 2 – метавулканиты сортавальской серии, *3* – метапсаммиты ладожской серии, *4* – мезопротерозойские граниты рапакиви Салминского массива, *5* – разрывы первого этапа, *6* – разрывы второго этапа, *7* – тренды систем интерференционной складчатости, *8* – государственная граница. Буквами в кружках обозначены: К – Карельский массив, М – зона Мейери; куполовидные выступы фундамента: Н – Хавус, I – Импилахти, Р – Путсари, S – Сортавальский. (*c*) – концептуальная блок-диаграмма тектонического строения территории Приладожья: *1* – гранитогнейсы архея, *2* – метавулканиты сортавальской серии, *3–5* – метапсаммиты ладожского комплекса в разных метаморфических фациях, *6* – интрузивные формации свекофеннского этапа тектогенеза, *7* – изограды метаморфизма, *8* – тектонические швы, *9* – разрывные нарушения, *10* – направления тектонического транспорта геоматериала.

[Morozov, 1999, 2002]. It should be noted that the tectonic deformations occurred there in the "basement-cover" system, and the Svecofennian structures were formed both in bedded formations of the Paleoproterozoic supracrustal cover and Archean granite-gneiss basement. In the latter, these structures were identified through their imposition on the systems of basite dykes intruded into the Archean cratonized substrate during the very first Svecofennian tectogenetic events and participated in its rheomorphism later on. These dykes are considered comagmates [Sudovikov et al., 1970] and supply channels for metavolcanites of the Sortavala series and, tectonically, zero structural benchmark for identification of the Svecofennian deformations in the Archean basement.

3. VEINED FORMATIONS IN POLYSTAGE STRUCTURAL PARAGENESES

3.1. Structural position of veined bodies

Integral elements in structural parageneses of each of the three stages identified and dated [Morozov et al., 2018] are different veined bodies, generally determining the position of shear fractures and the regional-deformation ellipsoid's compression – extension axes orientations. In low-temperature metamorphic zones, these are primarily the quartz or quartz-feldspar veins, and in the zones of initial stage of granitization to mature stage of ultrametamorphism (sillimanite-muscovite and sillimanite-orthoclase subfacies) these are granitoid veins which vary in composition due to fluid regime evolution [Sedova et al., 2004].

The data presented here are only related to veined granitoid bodies developed within areal distributions of amphibolite and granulite facies in the Ladoga complex strip including the Meyeri zone of thrusts and its adjacent system of the Archean dome-shaped basement protrusions widely known as "mantled gneiss domes" of P. Escola [Escola, 1948]. Details on thermodynamic parameters of metamorphism and petrogenetic conditions in these two zones can be obtained from [Velikoslavinsky, 1972; Glebovitskii et al., 2002; Baltybaev et al., 2009; Kulakovsky et al., 2015]. We only note here that there was a general decrease in temperature from first to third deformation stage, responsible for steady change in rheological properties and rock deformation behavior from predominantly plastic at the beginning to viscous-brittle and brittle at the final tectogenetic stages.

The involvement in geochemistry of granitoid veins was caused by the necessity of identification of compatible deformation events in the basement and its overlying deposits within the Ladoga and Sortavala series. They served simultaneously as reference materials for geochronological dating of the deformation stages and were used to correlate them to similar formations in the cover on the basis of general geochemical marks.

Tectonic events of the first deformation stage (D1) in the region induced areal development in the basement-and-cover system of the northwest-striking overthrust nappe and folded structures, embedded in the regional flower-inspired structure and synchronous with the main mineral and chemical transformations that gave rise to the formation of regional metamorphic zonality (Fig. 1, c). These fold-thrust structures within the dome-like basement protrusions, which also involved the metamorphosed basite dykes (Havus protrusion), appeared to be paragenetically related to granite veins separated along the thrust-fault planes and axial planes of synchronous folds (Fig. 2). The concordant age of zircons from these veins is 1870±6 Ma [Morozov et al., 2018].

Another similar example of the first-stage deformations is related to the Impilakhtin protrusion (Fig. 3, a), wherein basite dykes are deformed into large mapped isoclinal folds, initially lying, whose axial surfaces are conjugated with the systems of long granite veins (Fig. 3, b). Their structural analogues in the overlying metavolcanites of the Sortavala series are similarly foliated plagiogranite bodies oriented obliquely to dominating substrate stratification and to the contact with the Archean granite-gneisses, precisely in accordance with the position of shear fractures in the formation of compatible thrust structures (Fig. 3, c; 4, a). The age of these granite bodies turned out to be similar to the dates for the Havus veins mentioned above – 1859.4±8.5 Ma [Morozov et al., 2018].

Subsequently, these first-stage-deformation granite veins were folded in the hinge zones of the straight second-stage-deformation (D2) folds (see Fig. 3, a; Fig. 4, b)

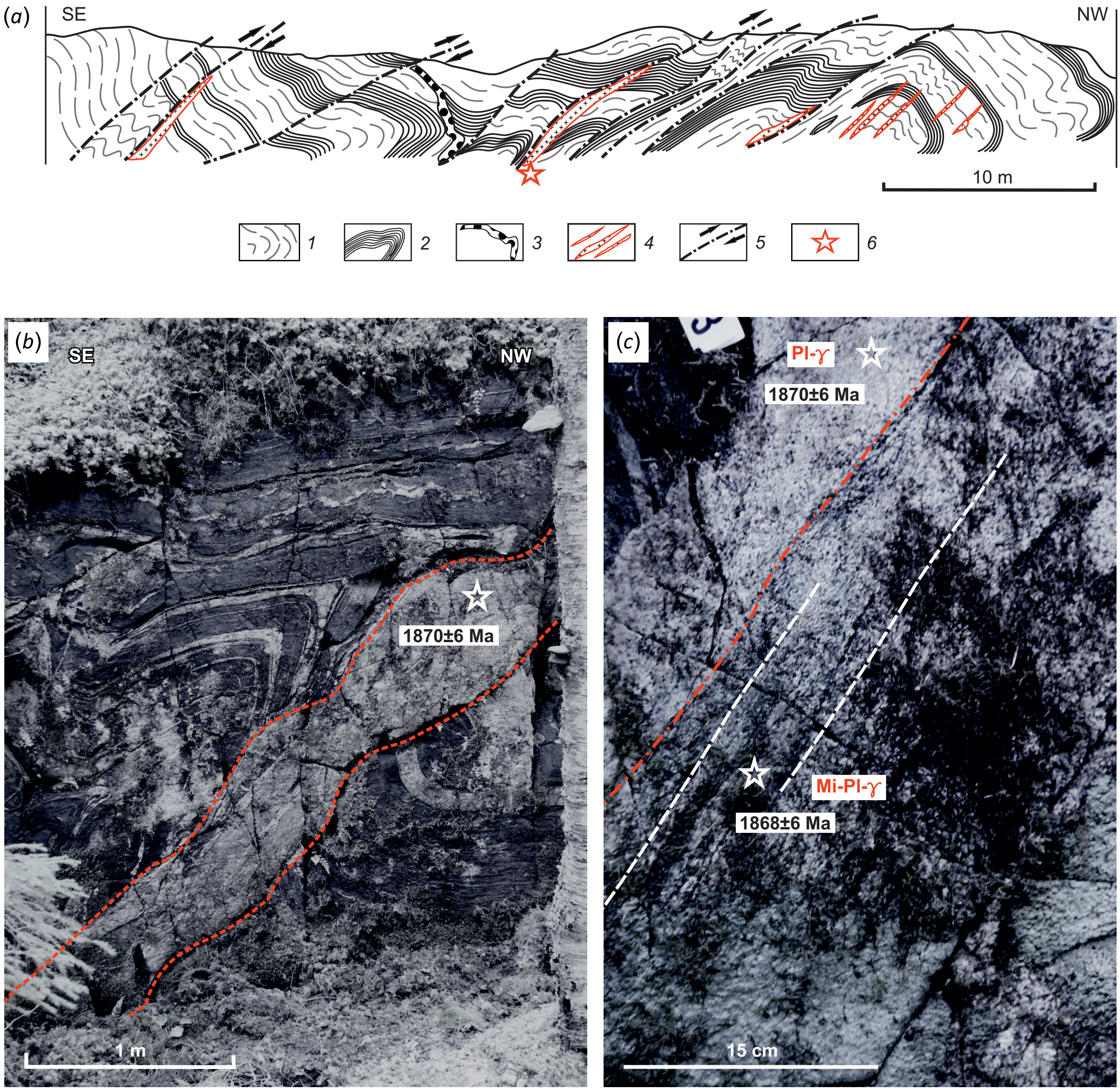

Fig. 2. Elements of the internal structure of the dome-shaped Havus protrusion.
(*a*) – fold-thrust system of the early Svecofennian tectogenesis in the Archean granite-gneissic substrate (an outcrop sketch): *1* – Archean granite-gneisses, *2* – metamorphosed basite dikes, *3* – early plagiogranite veins, *4* – partially gneissized and microclinized plagiogranite veins, *5* – thrust surfaces, *6* – plagiogranite sampling site; (*b*) – plagiogranite veined body in the thrust plane (ЛВ-1703/2); (*c*) – zone of superimposed foliation and microclinization in the plagiogranite vein (ЛВ-1703/1).

Рис. 2. Элементы внутреннего строения куполовидного выступа Хавус.
(*a*) – система складчато-надвиговых структур раннего этапа свекофеннского тектогенеза в архейском гранитогнейсовом субстрате (зарисовка обнажения): *1* – гранитогнейсы архея, *2* – тела метаморфизованных даек базитов, *3* – плагиогранитные жилы ранней генерации, *4* – частично огнейсованные и микроклинизированные жилы плагиогранитов, *5* – поверхности надвигов, *6* – место отбора пробы плагиогранита; (*b*) – жильное тело плагиогранита в надвиговой плоскости (ЛВ-1703/2); (*c*) – зона наложенного рассланцевания и микроклинизации плагиогранитной жилы (ЛВ-1703/1).

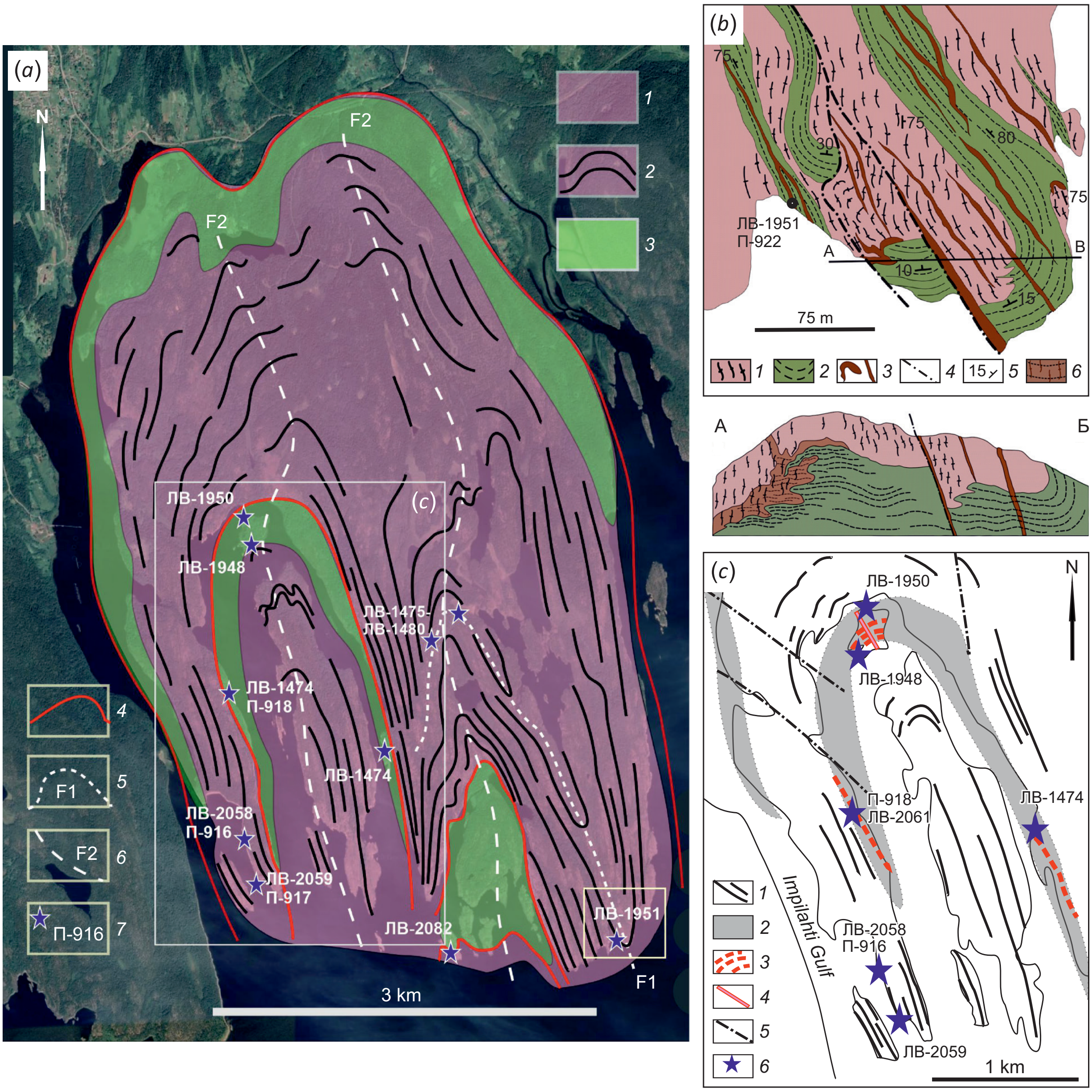

Fig. 3. Elements of the internal structure of the Impilahti basement protrusion.
(*a*) – a simplified structural-geological map of the protrusion: *1* – granite-gneisses of the Archean basement, *2* – Paleoproterozoic metamorphosed basite dikes in the granite-gneiss substrate, *3* – metavolcanics of the Sortavala series, *4* – tectonic contacts, *5–6* – axes of folds of the first (F1) and second (F2) generations in the structure of the Svecofennian granite-gneisses, *7* – sampling sites. Rectangles mark areas of detailed sampling; (*b*) – a scheme and a structural profile of the hinge zone of the first-generation Kulkhoniemskaya fold: *1* – granite-gneisses, *2* – metabasite dikes, *3* – granite veins of the first generation, *4* – faults, *5* – elements of layering, *6* – late pegmatoids; (*c*) – a scheme of the second-generation Haukkasari synform: *1* – metabasite dikes in the granite-gneiss substrate, *2* – metavolcanic rocks of the Sortavala series, *3* – plagiogranite veins of the first generation, *4* – veins of microcline-plagioclase granites of the second generation, *5* – faults, *6* – sampling sites.

Рис. 3. Элементы внутреннего строения Импилахтинского выступа фундамента.
(*a*) – упрощенная структурно-геологическая карта выступа: *1* – гранитогнейсы архейского фундамента, *2* – палеопротерозойские метаморфизованные дайки базитов в гранитогнейсовом субстрате, *3* – метавулканиты сортавальской серии, *4* – тектонические контакты, *5–6* – оси складок первой (F1) и второй (F2) генерации в свекофеннской структуре гранитогнейсов, *7* – точки отбора проб. Прямоугольниками отмечены участки детального опробования; (*b*) – схема и структурный профиль замковой части Кулхониемской складки первой генерации: *1* – гранитогнейсы, *2* – метаморфизованные дайки базитов, *3* – гранитные жилы первой генерации, *4* – разрывы, *5* – элементы залегания расслоенности, *6* – поздние пегматоиды; (*c*) – схема Хауккасарской синформы второй генерации: *1* – метаморфизованные дайки базитов в гранитогнейсовом субстрате, *2* – метавулканиты сортавальской серии, *3* – плагиогранитные жилы первой генерации, *4* – жилы микроклин-плагиоклазовых гранитов второй генерации, *5* – разрывы, *6* – места опробования.

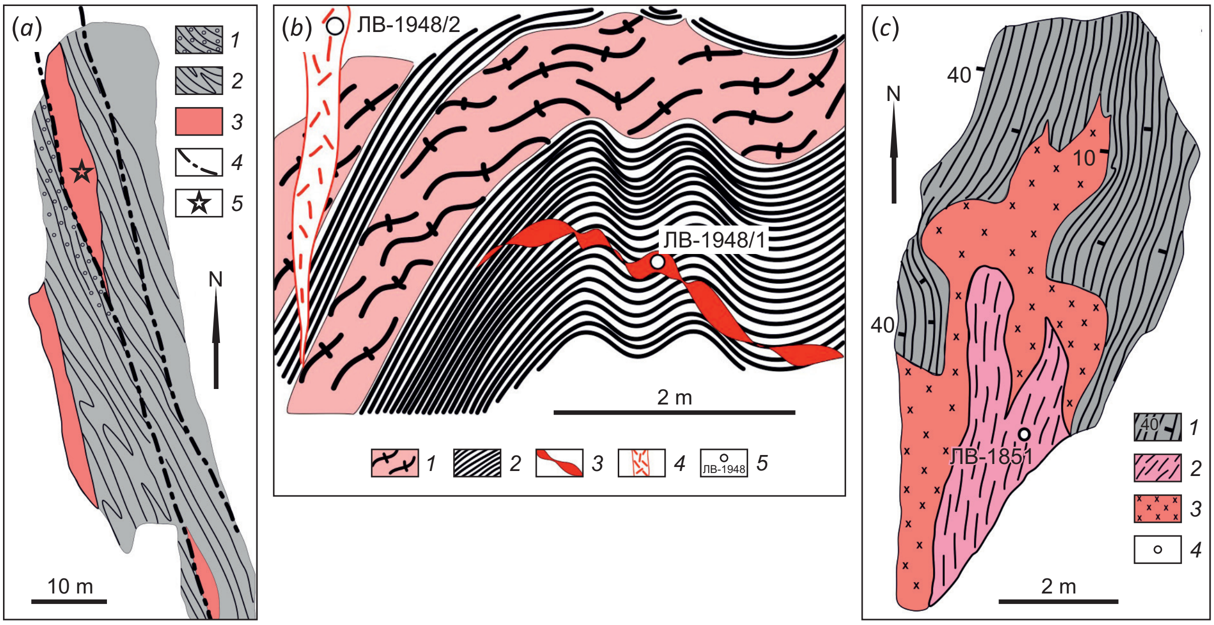

Fig. 4. Sketches of outcrops of granite-vein sampling.
(*a*) – early-generation granite veins in metavolcanics of the Sortavala series (point ЛВ-1474 on the eastern limb of the Haukkasaari synform): *1* – gabbro-amphibolites, *2* – banded amphibolites, *3* – granite veins, *4* – faults, *5* – sampling site; (*b*) – veins of two generations in hinge zone of the Haukkasari synform (point ЛВ-1948): *1* – granite-gneisses, *2* – metamorphosed basite dikes, *3* – first-generation plagiogranite vein, *4* – second-generation granite-pegmatite vein, *5* – sampling sites; (*c*) – vein injections in metavolcanic rocks around the Putsaari protrusion (point ЛВ-1851): *1* – metavolcanics of the Sortavala series, *2* – foliated granite vein, *3* – pegmatoid, *4* – sampling point.

Рис. 4. Схематизированные зарисовки обнажений опробования гранитных жил.
(*а*) – гранитные жилы ранней генерации в метавулканитах сортавальской серии (точка ЛВ-1474 на восточном крыле Хауккасарской синформы): *1* – габбро-амфиболиты, *2* – полосчатые амфиболиты, *3* – гранитные жилы, *4* – разрывы, *5* – место опробования; (*b*) – жилы двух генераций в замке Хауккасарской синформы (точка ЛВ-1948): *1* – гранитогнейсы, *2* – метаморфизованные дайки базитов, *3* – плагиогранитная жила первой генерации, *4* – гранит-пегматитовая жила второй генерации, *5* – места опробования; (*c*) – жильные инъекции в метавулканитах обрамления выступа Путсари (точка ЛВ-1851): *1* – метавулканиты сортавальской серии, *2* – рассланцованная жила гранитов, *3* – пегматоид, *4* – точка опробования.

whose axial surfaces correspond to a new generation of northwest- or submeridionally striking veins composed of microcline-plagioclase (ЛВ-1948/2 in Fig. 4, b, and ЛВ-1851 on Fig. 4, c). In the last site, their zircon dating yielded ages of about 1830 Ma (1827.9±4.9; 1828.1±4.9 Ma), determining the second-stage deformations of the Svecofennian tectogenesis.

The third deformation stage (D3), responsible for the formation of the northeast-oriented discrete folded and faulted structures, manifested itself through superimposed schistosity zones in the early-generation granite veins (Havus protrusion, point ЛВ-1703/1, Fig. 4, c), where the hosted zircons had newly formed outer shells whose SHRIMP-II dating yielded ages between 1772.2±4.7–1768.5±6 Ma [Morozov et al., 2018]. These transformations under conditions of low-temperature diaphtoresis in the epidote-amphibolite and greenschist facies reflected, to our mind, the events of already started orogenic stage.

Particular emphasis was given to rheomorphic veined bodies immediately in the granite-gneiss substrate of the Impilakhti basement protrusion (point П-916 in Fig. 3, a, c; Fig. 5). The originally Archean substrate usually persists there in the form of small isolated parts of micaceous gneisses (index 1 in Fig. 5) among shadow granite-gneisses, occasionally showing the elements of planar structure (index 2) but usually replaced almost completely by medium-grained granite substrate with massive texture (index 3). The absence of clearly defined boundaries and the presence of gradual transitions between these varieties imply an extensive impregnation of the substrate with granite-forming fluids. The dykes originally composed of basite rocks contain the records of both injective intersection veined bodies and elements of metasomatic substrate transformation, first by plagiogranite and then by microcline-containing material, and sustainable deoxidation of substrate in localized deformation zones and en echelon shear fractures. The final stages of development of these processes are marked by formation of pegmatoid veinlets and stringers which, regarding their en echelon system, were clearly controlled by the northeast-striking strike-slip faults of the third deformation stage (index 4, Fig. 5).

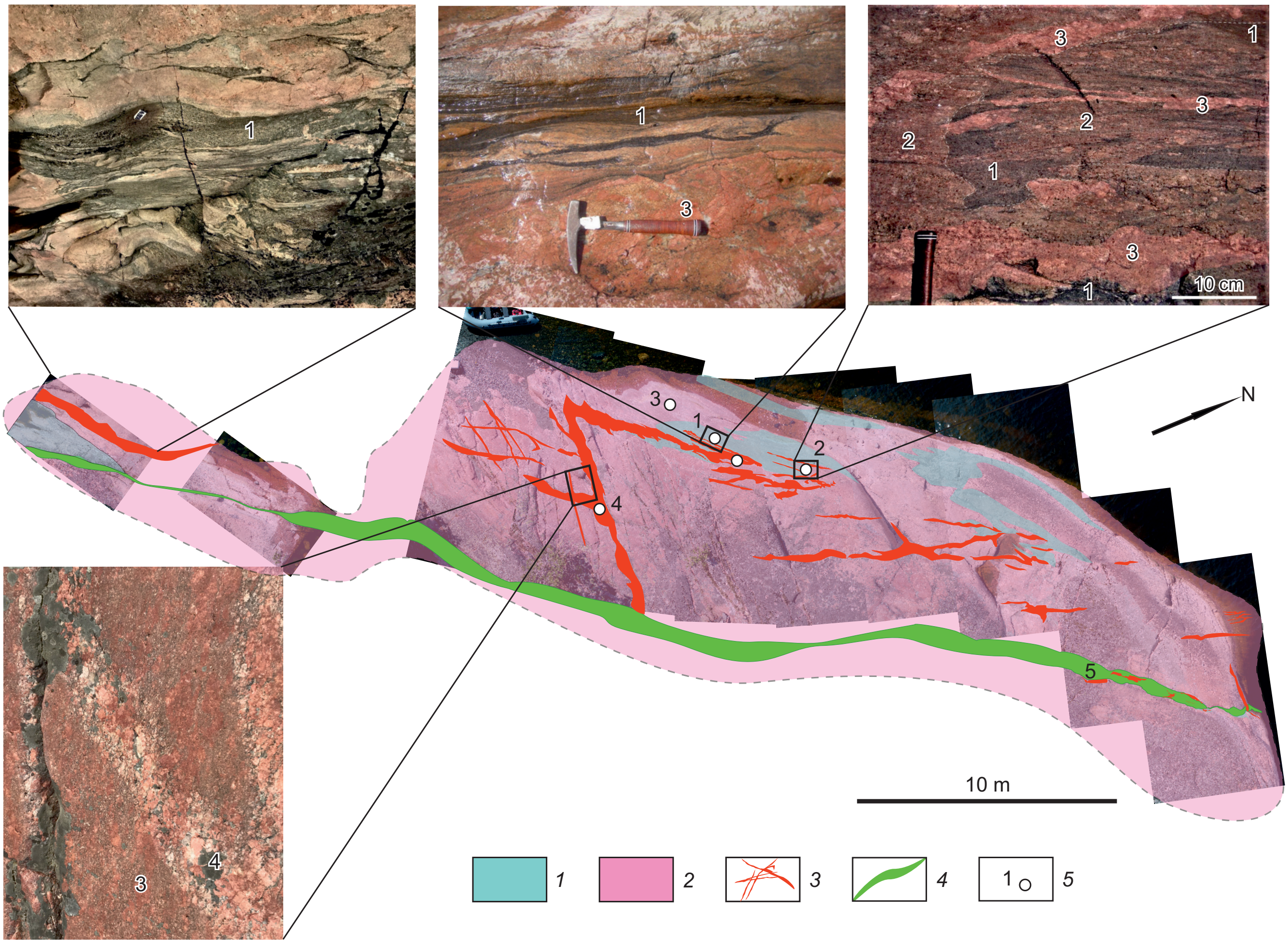

Fig. 5. The Svecofennian rheomorphism processes in the Archean granite-gneiss substrate (Impilahti protrusion, site П-916).
1 – relics of mica gneisses of the Archean age, *2* – granitized gneisses, *3* – segregations of pegmatoid veins, *4* – metabasite dykes, *5* – granitized rocks sampling sites. The numbers on the photo and on the diagram (corresponding to П-916 sample numbers) are: 1 – original mica gneisses, 2 – shadow banded granite-gneisses, 3 – massive granite, 4 – pegmatoid.

Рис. 5. Проявление процессов реоморфизма свекофеннского этапа в архейском гранитогнейсовом субстрате (выступ Импилахти, точка П-916).
1 – реликты слюдистых архейских гнейсов, *2* – гранитизированные гнейсы, *3* – жильные обособления пегматоидного состава, *4* – метаморфизованная дайка базитов, *5* – точки опробования гранитизированных разностей. Цифрами на фото и схеме обозначены (соответствуют номерам пробы П-916): 1 – исходные слюдистые гнейсы, 2 – теневые полосчатые гранитогнейсы, 3 – массивный гранит, 4 – пегматоид.

3.2. Geological-petrographical description of veined bodies

The studied granite-pegmatoid veins have the shape of stringers from a few centimeters to 50 cm, less often to 1.5–5.0 m thick (Fig. 6). Sometimes they look like orthotektites which compose irregularly shaped "spots" or lenses 20–30 cm in diameter. Less frequent occurrences are lenses encountered in two mutually perpendicular directions. Granites and their varieties are strongly leucocratic, with a biotite content of no more than 2–5 %. A typical feature of granitoids is that they vary from coarse-grained to pegmatoid. Worthy of note is the frequent occurrence of biotite rims at the boundary between pegmatoid lenses and their host rocks which, according to [Mehnert, 1971], testifies to the formation of these rocks through in situ melting. Most of the granites compose intersecting veins, partly formed under brittle deformation conditions. The granites and their host rocks contain accessory minerals of the same composition.

Granitoid veined bodies, according to a thin-section study, were subdivided into several petrographic varieties; biotite shadow plagiomigmatites, charnokites, leucocratic granites, orthotektites, and muscovite-quartz pegmatite-like rocks. They all have granoblast, somewhere hypidiomorphic-granular structure, with the traces of deformation observed therein but to a different extent, up to cataclastic structure. Alongside with the most typical 1–2 mm grains, these rocks are represented by fine (less than 0.1–0.2 mm)

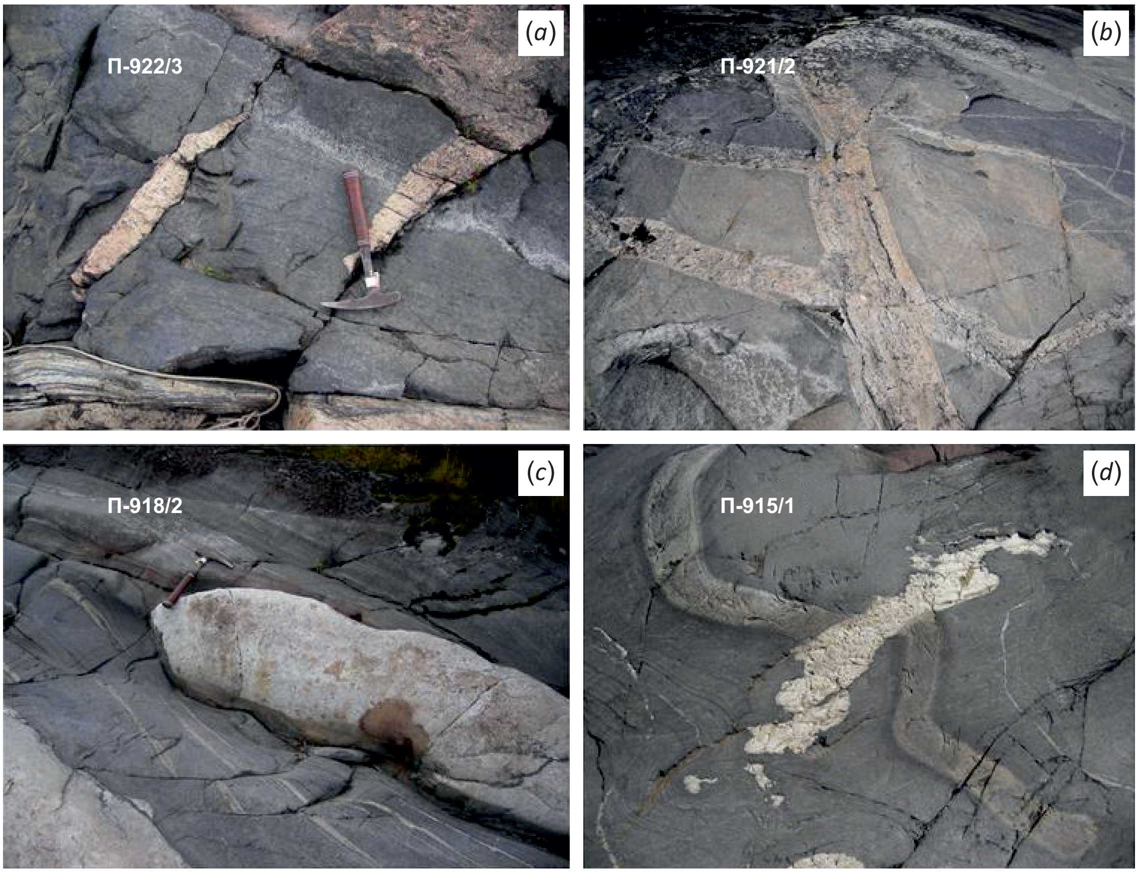

Fig. 6. Typical granitoid veins of different generations (the indicated numbers correspond to the numbers in App. 1, Tables 1.1, 1.2).

Рис. 6. Фотографии типичных гранитоидных жил разных генераций (указанные номера проб соответствуют номерам в Прил. 1, табл. 1.1, 1.2).

plagioclase grains with jagged margins, as if squeezed between coarser grains. There also occur flattened coarse plagioclase grains, vanishing unevenly in the form of spots, and curled biotite. Quartz grains are also distributed irregularly, ranging in size from fine subisometric or irregular grains in iterstitions to lenticular occurrences up to 7–3 mm in size. Quartz does not show any traces of deformation and might have been recrystallized after the stage of cataclastic and mylonitic rock formation. Quartz constitutes from 20 to 50 % of the bulk. Strong silicification leads to the occurrence of some amount of muscovite in the form of narrow plates up to 2–3 mm long. Such granites might be related to the areas of acid leaching as their axial parts. Among the vein-host rocks, there are observed relic sites of amphibole-biotite and biotite plagiomigmatites containing 5–10 % of biotite. Original substrate relics are also identified therein by the presence of irregularly shaped sites of "old" saussuritized plagioclase. All these data, as well as somewhat irregular distribution of microcline in rocks, testify to in situ formation of veins. The traces of blasocataclasis and partial mylonitization show the occurrence of brittle deformations at the final stages of this veined rock development.

4. GEOCHEMISTRY OF VEINED BODIES AND HOST ROCKS

4.1. Research methods

On the sites described above, the samples were taken from both veined bodies of all three deformation stages (23 samples) and their host rocks (11 analyses) (Table 1). Petrogenic element analyses were performed by Bruker AXS S4 Pioneer XRF spectrometer (Germany) in the laboratory of the Geological Institute (GIN) RAS, and microelement analyses were performed by "Element 2" High Resolution ICP-MS system (Thermo Fisher Scientific of GmbH, Germany), at the same place. The results were checked using standard schist sample SBC-1 (USGS, USA) and reference rhyolite sample ORPT-1 (IAG, Great Britain) analysis. The obtained concentrations differed from the attested by no more than 10–15 RLT. %. The methods are described in more detail in [Okina et al., 2016].

4.2. Geochemical evidence

Geochemical study of 23 sampled veined bodies showed a well-defined set of negative Eu anomalies typical for granites whereas some dykes or veins, similar in appearance, are characterized by a positive Eu anomaly (Fig. 7).

Table 1. Comparison between the groups of geochemical samples of pegmatoid granitoids and structural and compositional complexes, initial rocks and stages of deformation in the Northern Ladoga region

Таблица 1. Группы сопоставления геохимических проб пегматоидных гранитоидов со структурно-вещественными комплексами, исходными породами и этапами деформаций в Северном Приладожье

Structural and compositional complexes	Source rocks	Deformation stages		
		D1	D2	D3
Ladoga series (amphibolite and granulite facies)	П-920/1 П-97/2 П-915/2 П-927/2	П-927/3 П-915/1 ЛВ-1946/4	П-920/2	П-97/2 ЛВ-1742/2 ЛВ-1875/2
Sortavala series and dykes (supply channels) (amphibolite facies)	П-917/1 П-918/1 П-922/1 П-926/1	П-922/1 П-926/2 ЛВ-1951 ЛВ-1948/1	П-917/4 П-918/2 ЛВ-1851 ЛВ-1948/2 ЛВ-1950	–
Archean basement	П-99/1 П-916/1 П-921/1	П-916/3 ЛВ-1703/2	П-921/2 П-916/4	П-99/2 П-916/2 ЛВ-1703/1

Note. Source rocks – 11 samples, granitoid veins – 23 samples.

Примечание. Исходные породы – 11 проб, гранитоидные жилы – 23 пробы.

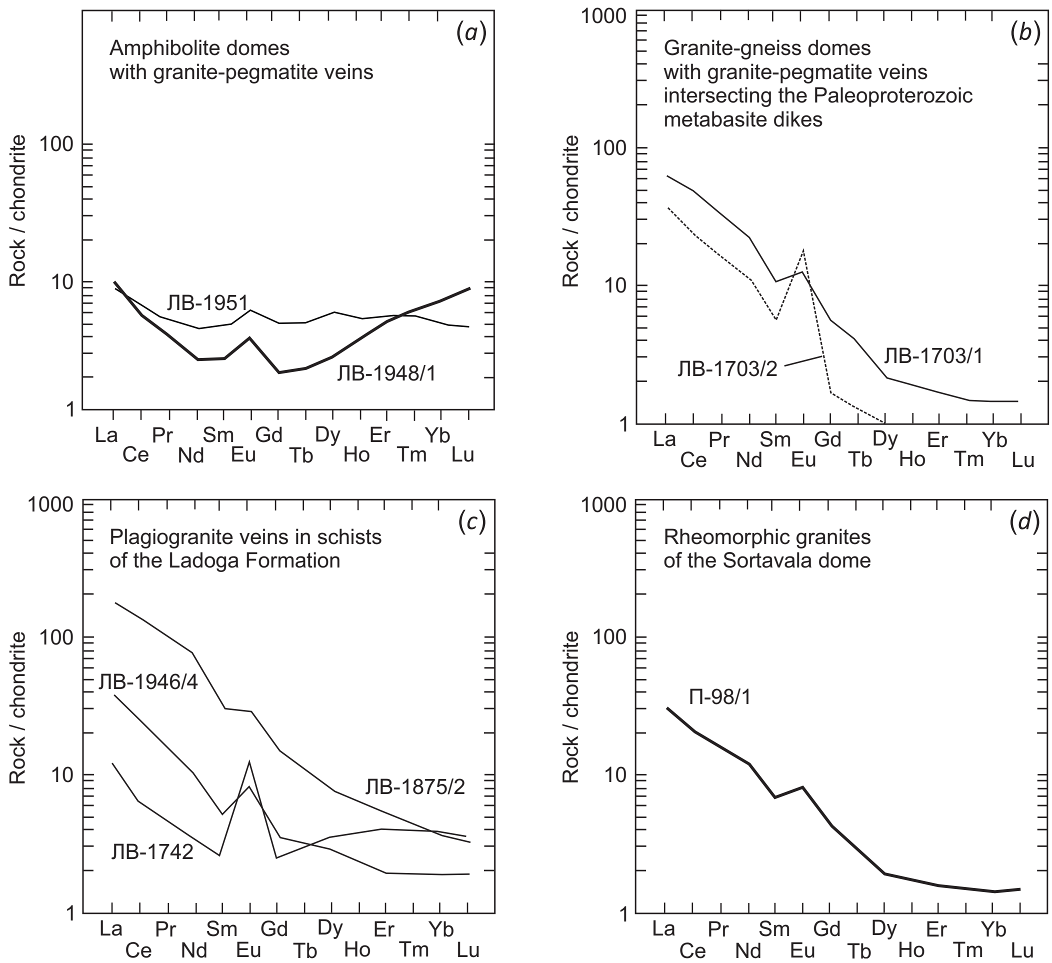

Fig. 7. Representative examples of chondrite-normalized plots of REE distribution with a positive Eu anomaly in granite veins from different structural and compositional complexes in the Northern Ladoga region. Sample numbers correspond to point numbers on the maps and sample numbers in Table 1 and App. 1, Table 1.1.

Рис. 7. Представительные примеры нормированных по хондриту графиков распределения REE с положительной Eu-аномалией в жильных гранитах из разных структурно-вещественных комплексов Северного Приладожья. Номера проб соответствуют номерам точек на картах и номерам проб в табл. 1 и Прил. 1, табл. 1.1.

This anomaly is rather uncommon in acid rocks and might be indicative of unique formation conditions.

4.3. Geochemical features of veined bodies and their host complexes

Our studies in the Northern Ladoga show that the veined granite rocks with positive Eu-anomalies are common not only among grey gneisses and rheomorphic dome-shaped protrusion cores but also among their bordering complexes (amphibolites of Sortavala series), schists of the interdomal spaces (Ladoga series), and granulites occurring south of the protruding zone.

Petrogeochemistry of acid rocks with a positive Eu anomaly. All studied rocks with a positive Eu anomaly, irrespective of their confinedness to different structural and compositional complexes, are characterized by wide-range (from 64 to 75 %) SiO_2 content and high alumina content. The highest silica content is observed in the rocks which experienced acid leaching. The latter show evidence of an extreme depletion in potassium (K_2O=0.35–0.58 wt. %) and most of the microelements. These are so called exhausted granites. However, most of the rocks studied are characterized by high potassium contents reaching anomalously high values in some of the samples which evidently imply metasomatic supply of this element (App. 1, Tables 1.1 and 1.2).

A feature of the rocks considered is the depletion in such components, as TiO_2, Fe_2O_3, MnO, MgO, P_2O_5, as a result of which they are leucocratic and, based on alkali-silica ratio, mostly related to subalkaline granites. Most of the samples correspond to leucogranites and subalkaline leucogranites (Fig. 8). The same figure shows composition fields of rock series, with the points of veined-granite compositions fallen within the fields of alkaline and calc-alkaline series.

A more ambiguous distribution of images of the granitoid analysis data points is observed in the CaO/Na_2O–Al_2O_3/TiO_2 diagram [Sylvester, 1998] (Fig. 9), drawn on purpose to identify the sources of granitoid melt. The scattered images of the graitoid points imply that these rocks (unlike, for example, the rocks of the Matkaselsky granite complex of the Northern Ladoga region, Field II on Fig. 9) are not magmatic but formed on different substrates under the influence of the same-type fluid (as will be discussed below).

Table 1.1 shows chemical compositions of typical veined bodies located both in the Ladoga series, occupying the interdomal space, and the protrusions with their amphibolite framing. Implying that the veins studied were metasomatically formed in situ under the fluid influence, we present Tables 1.2, 1.3 and 1.4, which, along with the veined bodies, show the host rocks that makes it possible to determine what elements were supplied or withdrawn during these veins' formation. In all cases, the granites with a positive Eu anomaly are characterized by depletion of Sc, V, Cr, Co, Ni, Cu, Y, Zr, Nb, Hf and REE relative to the host rocks. Some elements have an alternating-sign ratio, i.e. they undergo withdrawal in some cases and supply in others. These are Li, Be, Ga, Rb, Sr, Sn, Cs, Tl, and Th. However, there is a group of elements showing significant supply. These are Mo, Sb, Ba, W, Pb, and U. Only in one case, related to veined rocks among the granulites, there occurs a supply of LREE and Eu, whereas other cases show complete withdrawal of REE and incomplete withdrawal of Eu, owing to which there is a formation of a positive Eu anomaly. It would be interesting to compare what occurs during the formation of granites with a negative Eu anomaly (see App. 1, Table 1.3). The rocks also become leucocratic though microelements behave somewhat differently. Only chalcophile elements – V, Cr, Co, Ni, Cu и Y – unambiguously tend to be withdrawn. All others are characterized by alternating-sign states. Special emphasis should be put on the behavior of W and Ba which

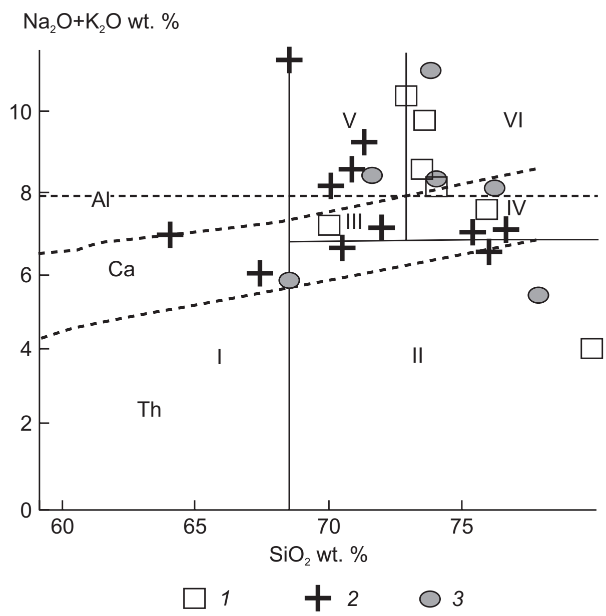

Fig. 8. An alkali-silica diagram.
1 – veined granitoids with a negative Eu anomaly, granitoids with a positive Eu anomaly; *2* – veined bodies; *3* – blastomylonites and shadow granites. I – tonalites, II – plagiogranites, III – granites, IV – leucogranites, V – subalkaline granites, VI – subalkaline leucogranites. Composition fields of granitoids series (dotted lines) – Al – alkaline, Ca – calc-alkaline, Th – tholeiitic – are drawn after [Martin, 1999].

Рис. 8. Диаграмма суммы щелочей и кремнезема.
1 – жильные гранитоиды с отрицательной Eu-аномалией, гранитоиды с положительной Eu-аномалией; *2* – жильные тела; *3* – пластовые бластомилониты и теневые граниты. I – тоналиты, II – плагиограниты, III – граниты, IV – лейкограниты, V – субщелочные граниты, VI – субщелочные лейкограниты. Поля составов серий гранитоидов (пунктирные линии): Al – щелочных, Ca – известково-щелочных, Th – толеитовых, даны по [Martin, 1999].

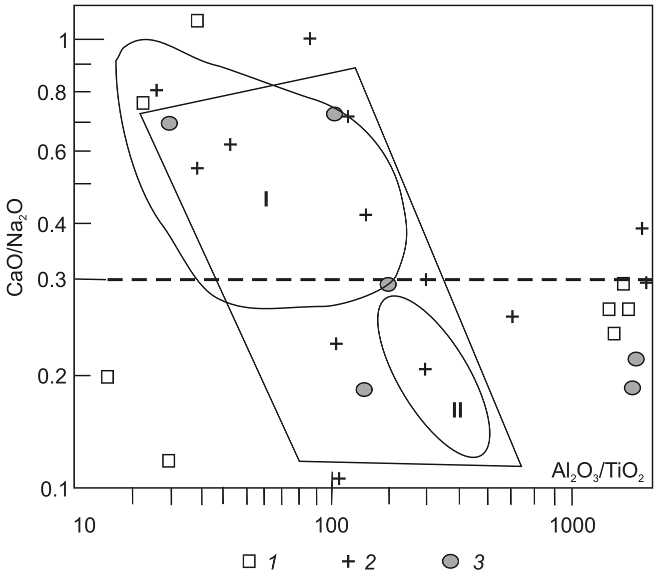

Fig. 9. Diagram CaO/Na$_2$O – Al$_2$O$_3$/TiO$_2$ [Sylvester, 1998] for post- and late orogenic granitoids of the Ladoga region.
Trapezium – composition field of post-collisional high-alumina granites. The dotted line separates granites with high (>0.3) and low (<0.3) CaO/Na$_2$O ratios, which roughly corresponds to experimental melts obtained by anhydrous melting of metagraywacke and metapelitic rocks. *1* – veined granitoids with a negative Eu anomaly; *2* – veined granitoids with a positive Eu anomaly; *3* – blastomylonites and shadow granite-gneisses. Fields I and II – late orogenic and post-orogenic granitoids of the Ladoga region, respectively [Sharov, 2020].

Рис. 9. Диаграмма CaO/Na$_2$O – Al$_2$O$_3$/TiO$_2$ [Sylvester, 1998] для пост- и позднеорогенных гранитоидов Приладожья.
Трапеция – поле составов постколлизионных высокоглиноземистых гранитов. Пунктирная линия разделяет граниты с высоким (>0.3) и низким (<0.3) отношением CaO/Na$_2$O, что приблизительно соответствует экспериментальным расплавам, полученным при безводном плавлении метаграувакковых и метапелитовых пород. *1* – жильные гранитоиды с отрицательной Eu-аномалией; *2* – жильные гранитоиды с положительной Eu-аномалией; *3* – бластомилониты и теневые гранито-гнейсы. Поле I – позднеорогенные и поле II – посторогенные гранитоиды Приладожья [Sharov, 2020].

experience unambiguous withdrawal. As this takes place, light rare earth elements are supplied and medium-heavy and heavy rare earth elements are withdrawn.

All REE are trivalent, with Eu^{+++} transformed into Eu^{++} in reducing environment in accordance with [Balashov, 1989]. Therefore, during melting or metasomatic replacement under the influence of reduced fluids (hydrogen or hydrocarbon), there is a predominant formation of Eu^{++}. Eu^{++} is capable of accessing the positions inaccessible to Eu^{+++}. That is why feldspars can be added more easily by Eu^{++}, which substitutes similarly-sized Sr^{++}, which, in its turn, substitutes Ca^{++}. In barium-bearing minerals, Eu^{++} substitutes Ba^{++} [Baturin, 2004]. Eu^{++} is larger than Eu^{+++} [Balashov, Tsoi, 1989], so besides the favorability of reduced fluids, Eu^{+++} transformation into Eu^{++} is also related to extensional environment which to our mind might also be important for geodynamic reconstructions.

Let us consider the behavior of some microelements related directly (Sr, Ba) or indirectly (Zr, Rb, Ca) to REE concentrations

Rubidium. Worthy of note is the depletion of accompanying elements, in particular rubidium, in the rocks studied whose rubidium content is 2–10 time lower than that of the lithospheric granite rocks [Beus, 1981]. However, the rubidium content of the studied granitoid samples approximates to the Clarkes (162 g/t versus 210 g/t) but these are isolated cases. There is no regularity in rubidium and potassium contents in the rocks, though the highest rubidium concentrations are typical of the rocks with anomalously high (8–9 wt. %) amount of potassium oxide. Generally, the depletion of rubidium in rocks may be attributed to their negligible biotite content, since it is known [Erlang, 1972] that rubidium is found in micaceous acid rocks rather than in rocks containing K-bearing minerals. In cases where the parent rock is granulite or amphibolite, the rubidium content of granites studied is higher than that of host rocks.

Zirconium. As in the case with rubidium, the studied rocks are depleted in zirconium whose concentrations are 2–10 times lower than the Clarkes for the granite, though unlike rubidium, the zirconium content therein is much lower than in the vein-host rocks. A study of granitization of the basic rocks involved the use of previously obtained correlation between zirconium and titanium [Shcherbakova, 1988]. Negligible titanium oxides in granites (prevalently 0.03–0.13 wt. %) and the lack of accessory zircon therein may produce low concentrations of both zirconium and REE. We would like to note sufficient withdrawal of Zr, TiO_2 and Y, i.e. the main components in the titanium-zirconium placers which over the last few years are supposed to have polygenic fluid-metasomatic genesis [Makeyev, Skublov, 2016].

Strontium and barium. The content of strontium in the granitoids studied is 1.5–6.0 times higher than the Clarkes of granites in the lithosphere, except for individual samples whose strontium content is close to the Clarkes (90–100 g/t versus 110 g/t) (see App. 1, Tables 1.1, 1.2). Strontium is characterized by isomorphic substitution with calcium in calcium-bearing minerals of magmatic rocks, mainly in plagioclases [Beus, 1981]. As seen in Fig. 10, a, the concentration of strontium in rocks increases with increasing calcium content. As in the case of barium, there is a direct relationship between the content of strontium in magmatic feldspars and the temperature of their formation [Makrygina, Petrova, 1996]. A specific feature of the distribution of barium is known to be its ability to accumulate in potassium-bearing minerals. The rocks studied (except for individual samples) have a very low content of biotite, and potassium feldspar is the only mineral that has a propensity

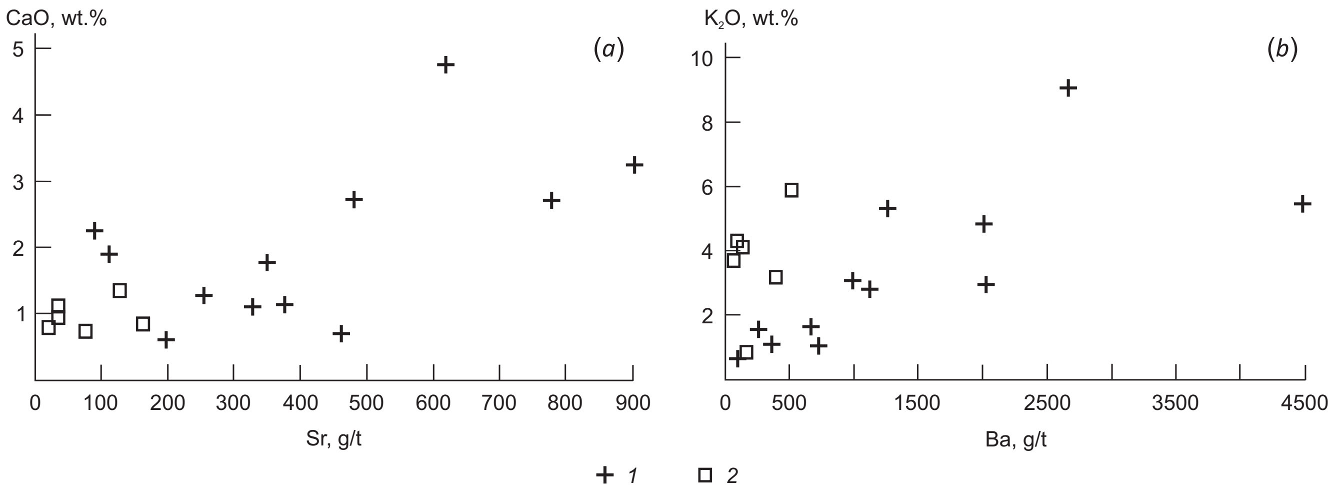

Fig. 10. Diagram of CaO–Sr (*a*) and K_2O–Ba (*b*) for acidic veined rocks in the Northern Ladoga region, having positive (*1*) and negative (*2*) europium anomaly.

Рис. 10. Диаграмма CaO–Sr (*a*) и K_2O–Ba (*b*) для кислых жильных пород Северного Приладожья, имеющих положительную (*1*) и отрицательную (*2*) европиевую аномалию.

to concentrate barium. However, the barium content of potassium feldspar in biotite granites of the Belomorye Belt (also showing a positive Eu anomaly) is 744 g/t [Shcherbakova, 1988], whereas the concentration of barium in rocks is often higher than that which implies it can also be present in other minerals, for example, in plagioclase. Barium content of veined granites varies over a wide range from 50 to 4480 g/t (see App. 1, Tables 1.1, 1.2). As shown in the tables, the content of barium in all samples, except for those with low K_2O contents, is much higher than that in the Earth's granite crust (830 g/t). There is a direct (though not strong) correlation between barium and K_2O contents of the rocks studied (Fig. 10, b). The lowest content of barium was recorded in the samples with K_2O contents no higher than 1 %, but the barium contents of the samples with K_2O contents higher than 5 wt. % are 1100, 1700 and 4480 g/t. However, the barium content of granites in all the cases is higher than that of host complexes. Therefore, the barium and especially strontium contents of the rocks considered are related to the contents of petrogenic host elements – potassium and calcium. High concentration of these elements in granites can be partially attributed to anomalously high temperature of granite formation which is confirmed by experimental data [Beus, 1981].

Rare-earth elements. The REE content of the rocks studied is very low (Fig. 11, 12). Except for two samples, all others have La, Ce, Nd and Sm contents 2–30 times lower than those in the Earth's granite crust. The granitoids under consideration are characterized by an even lower content of heavy REE whose concentrations in some of the samples are close to chondrite. Depletion of rare earth elements in the granites studied is particularly evident when compared to the host rocks (see Fig. 11), though the granites are often characterized by high $(La/Yb)_n$ ratios (>60). However, there is one more group of rocks with low $(La/Yb)_n$ ratios (1.2–2.5) attributed to high HREE contents, but it is very rare. High HREE contents of granites are most commonly due to HREE supply at final stages of the evolution of massifs. In our case, there are no HREE minerals. Current research shows that REE are often present in an intermolecular space, and that might be the case [Fadin et al., 2016]. There is no distinct relationship between a positive Eu anomaly and $(La/Yb)_n$ ratios (Fig. 13). However, the samples with negative values (Eu/Eu* less than 1) show the relationship between the anomaly size and REE differentiation degree, which indicates some differences in the character of crystallization of these two types of veined granites, probably related to different oxidation-reduction properties of fluids.

Low contents of heavy REE are related to leucocratization of the rocks which contain a very small amount of dark-colored minerals (1–10 %) and are represented primarily by biotite. Heavy-REE-bearing accessory minerals are not typical of the rocks studied either.

Fig. 14 shows that the presence of a negative Eu anomaly is related to a small amount of strontium, and the absence of the maximum Eu anomaly – to its largest amount which implies that not all Eu substitutes for strontium and can be found in some other place. The-rocks that contain an equal amount of CaO may have either positive or negative Eu anomaly. This implies that there is another factor of Eu concentration. The increase of CaO content is not accompanied by the development of Eu anomaly which implies that traditional ideas about substitution of Eu^{++} for strontium and that of strontium for Ca may not appear to match reality.

Pertogeochemistry of host rocks. The only available basic granulite sample (П-97/2) is typical of the Ladoga structure. Due to its low contents of Al_2O_3, K_2O $(La/Yb)_n$= =1.5, this rock is similar in composition to tholeitic basalt. These granulites are completely different from those of the Lapland type and are more similar to the granulites common among granite-gneisses of the Archean basement. The granite-gneiss basement rocks are represented by samples П-99/1, П-913/1 (Fig. 15, a), and П-916/1. These are typical representatives of "grey gneisses", with high Al_2O_3 and Sr concentrations and high $(La/Yb)_n$ ratios. Multiple lenses and differently thick layers of amphibole can be mapped in the domes. Samples П-914/1, П-918/1, П-922/2, and П-926 are similar in composition to typical tholeitic basalts with $(La/Yb)_n$ close to 1, though sample П-917/1 represents the rock which rarely occurs in this region. Due to numerous plagioclase phenocrysts, this rock is actually gabbro-anorthosite and shows a weak positive Eu anomaly (see Fig. 12). It is worthy of note that the granite dyke, intersecting this rock, has a negative Eu anomaly, i.e., no evidence is found for inheritance of this anomaly in the development of the granite vein. There are many examples of veins hosted by schists of the Ladoga series: П-915/2, П-920/1, П-922/3, and П-927/2. All these host rocks are similar to the detail-studied rocks from the Ladoga series cross-section [Myskova et al., 2012] and their composition is similar to that of PAAS, which is indicative of isochemical nature of their metamorphic transformations.

In the marginal part of the Impilakhtinsky basement protrusion (see Fig. 3, 5), the studies have been made on

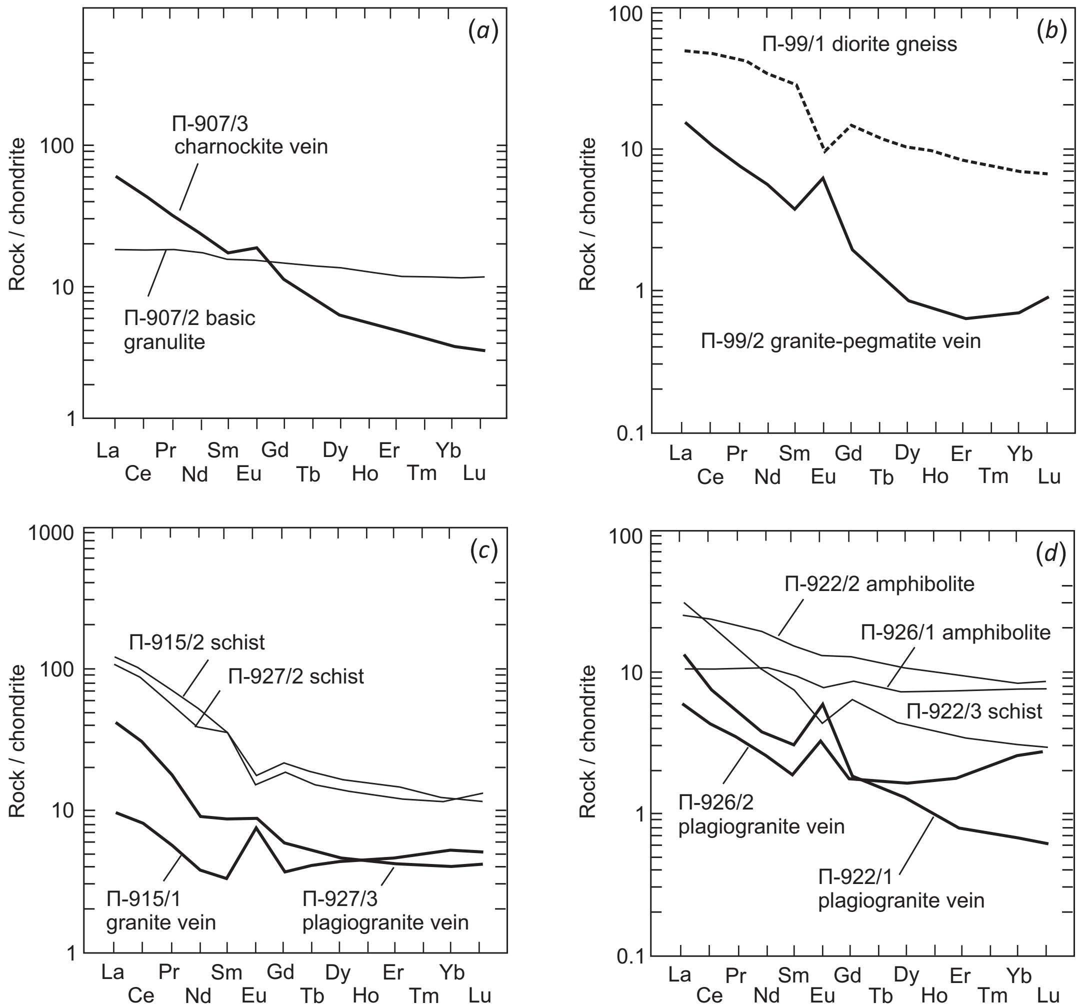

Fig. 11. Chondrite-normalized graphs of REE distribution in veined granites with a positive Eu anomaly and their host rocks in the Northern Ladoga region in different structural settings.
(*a*) – granulite field, (*b*) – granite-gneiss dome-shaped protrusion, (*c*) – schist interdomal infill (Ladoga series), (*d*) – amphibolite-schists horizons within granite-gneiss protrusions.

Рис. 11. Нормированные по хондриту графики распределения РЗЭ в жильных гранитах с положительной Eu-аномалией и вмещающих их породах Северного Приладожья в различных структурных обстановках.
(*a*) – гранулитовое поле, (*b*) – гранитогнейсовый куполовидный выступ, (*c*) – сланцевое «межкупольное» заполнение (ладожская серия), (*d*) – амфиболит-сланцевые горизонты внутри гранитогнейсовых выступов.

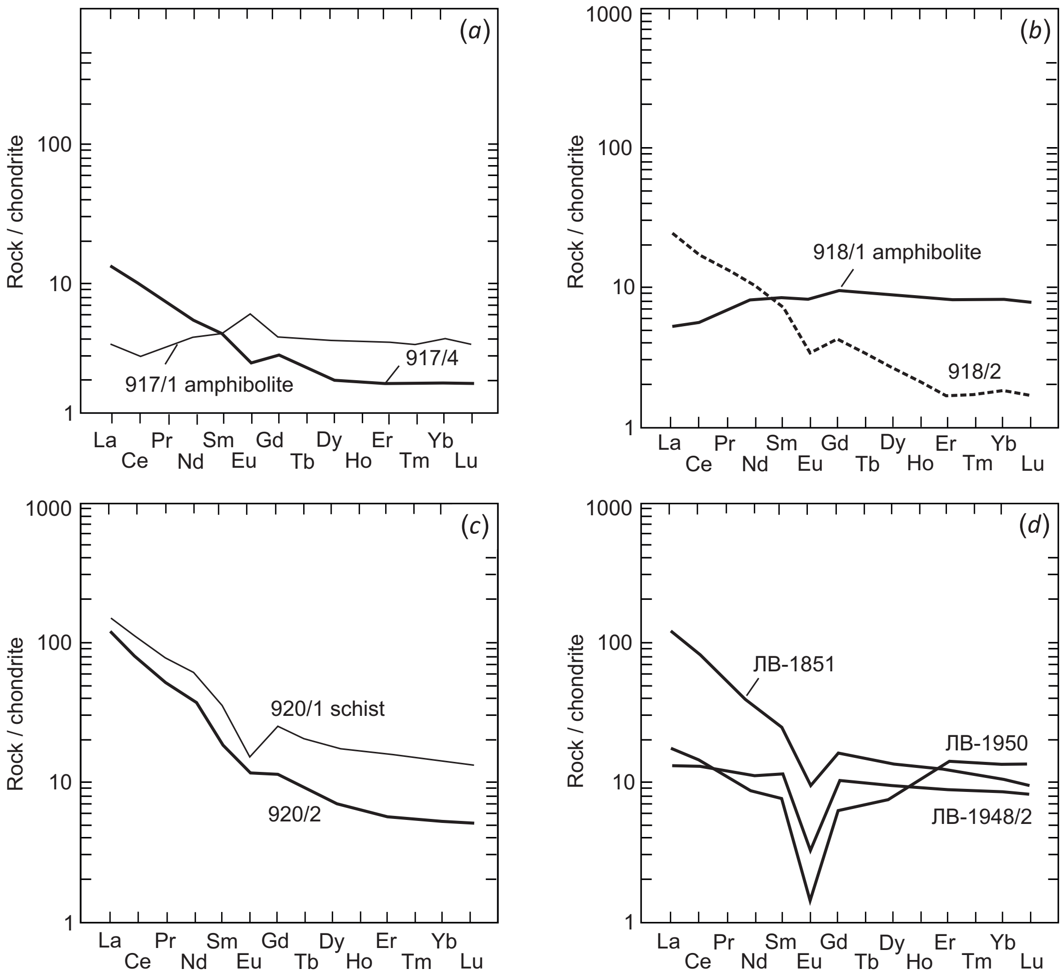

Fig. 12. Chondrite-normalized REE distributions in felsic veined rocks with a negative Eu anomaly and their host rocks in the Northern Ladoga region in different structural settings.
(*a*) and (*b*) – amphibolite bodies inside a granite-gneiss dome-shaped protrusion, (*c*) – interdomal space, (*d*) – amphibolite framing of protrusions.

Рис. 12. Нормированные по хондриту распределения РЗЭ в жильных кислых породах с отрицательной Eu-аномалией и вмещающих их породах Северного Приладожья в разных структурных обстановках.
(*a*) и (*b*) – в амфиболитовых телах внутри гранитогнейсового куполовидного выступа, (*c*) – «межкупольное» пространство, (*d*) – в амфиболитах обрамления выступов.

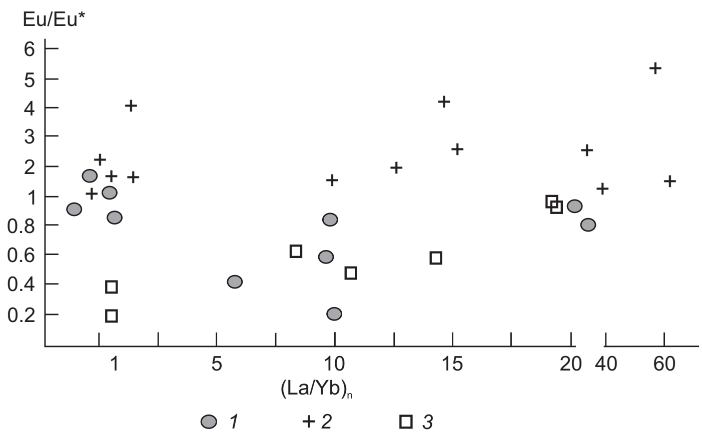

Fig. 13. Relationship between the europium (Eu/Eu*) anomaly magnitude and the REE differentiation degree $(La/Yb)_n$. *1* – host rocks; *2* – granites with a positive Eu anomaly; *3* – granites with a negative Eu anomaly.

Рис. 13. Зависимость величины европиевой (Eu/Eu*) аномалии от степени дифференциации REE $(La/Yb)_n$. *1* – вмещающие породы; *2* – граниты с положительной Eu-аномалией; *3* – граниты с отрицательной Eu-аномалией.

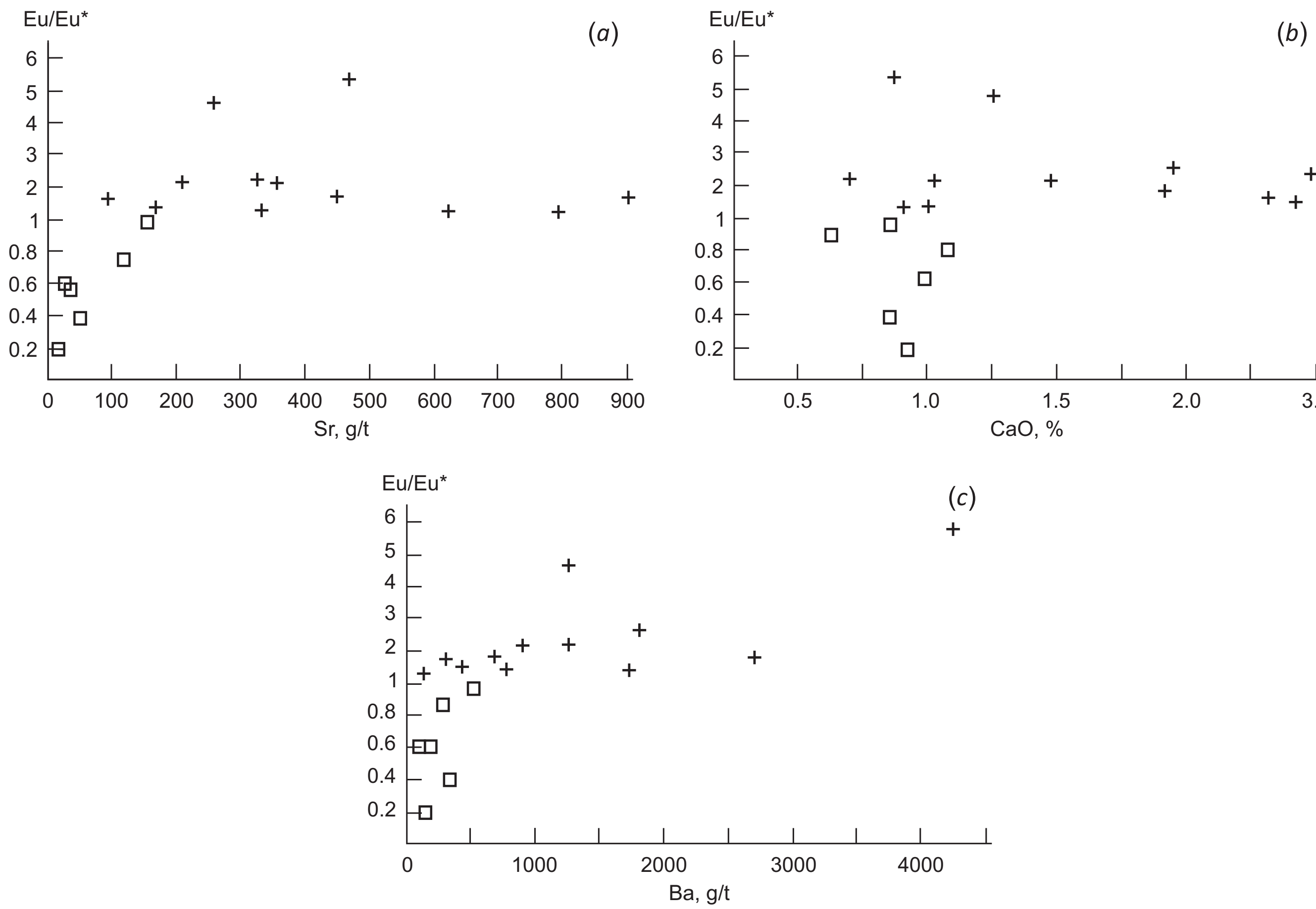

Fig. 14. The ratio of the europium anomaly (Eu/Eu*) to strontium (*a*), CaO (*b*) and barium (*c*) in the rocks studied. The legend is the same as in Fig. 13.

Рис. 14. Отношение европиевой аномалии (Eu/Eu*) к стронцию (*a*), CaO (*b*) и барию (*c*) в исследуемых породах. Условные обозначения те же, что и на рис. 13.

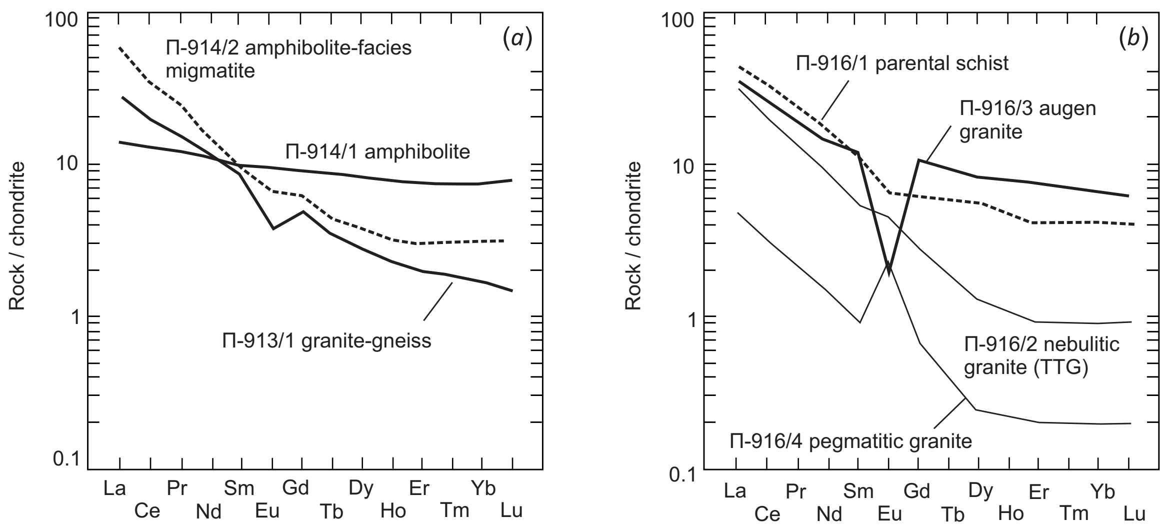

Fig. 15. Chondrite-normalized REE distribution in rocks from "dome-shaped" basement protrusions.

Рис. 15. Нормированное по хондриту распределение РЗЭ в породах из «куполовидных» выступов фундамента.

the series of differently granitized rocks (including those with the positive Eu anomaly), in which the microelement distribution is similar to that in veined bodies. Among the granitoids there are black-colored skialiths that geologically represent gneiss as a source rock (П-916/1) which contacts with migmatites. This gneiss has a typical REE distribution with $(La/Yb)_n$=18 and a weak negative Eu anomaly (0.86). The gneisses contact with shadowy granite (П-916/2) – a typical "grey" gneiss-granite with high $(La/Yb)_n$=32 and a weak positive Eu anomaly (1.35). The veined granite body (sample П-916/4) is composed of massive "red-meat" varieties, depleted in all elements as compared to shadowy granite-gneisses but rich in Ba and having the positive Eu anomaly (App. 1, Table 1.4). In contrast, sample П-916/3 – augen granite – has a well-defined negative Eu anomaly and, in spite of the presence of microcline and high potassium content, is extremely depleted in Ba (50 g/t) which is much lower than the Clarke. It is obvious that these rocks, with almost the same macroelement content, differ substantially in their texture (massive and directive – augen) which implies that the source rocks – "grey" gneisses – have different dynamics of changes in their properties (sample П-16/2). It is this local variability of dynamics determined by the compression-extension interaction mode that, in our opinion, controlled the fluid regime which, in its turn, provided for supply/withdrawal of microelements.

5. DISCUSSION AND INTERPRETATION OF DATA

Many scientists, referring to the experimental works [Balashov, Tsoi 1989; Beus, 1981; Taylor, McLennan, 1988], relate the anomalous Eu distribution to substitution of Eu^{++} for Eu^{+++} in the plagioclase structure, i.e. in the formation of granites with the positive Eu anomaly $Eu^{++} \leftrightarrow Eu^{+++}$ balance shifted toward divalent Eu. In accordance with this scheme, the Eu anomaly size is directly proportional to the potassium and strontium contents, but in our case (see Fig. 14, a, b) this phenomenon did not exist. It is worthy of note that the absence of correlation between a large positive Eu anomaly and strontium contents was also reported by other researchers [Norman et al., 1992]. In our case, the maximum positive Eu anomalies are typical of the granites high in Ba, i.e. in the element whose accumulation is often related to deep-seated fluid-saturated rocks: kimberlites, laproites, and sanukitoids [Terekhov, Baluev, 2011]. It is noted that Eu concentration in veined granites is lower than that in the amphibolite-facies metamorphic host rocks; on the contrary, the granites intersecting the rocks of the granulite association (already depleted in lithophile elements) have high Eu contents (see Fig. 11, a) which are also typical for such object as the Lapland Granulite Belt [Terekhov, Levitsky, 1993].

The granites, depleted in light REE and characterized by a clearly defined negative Eu anomaly, are rather abundant in nature. Light REE depletion, which occurs when granites originate by crystallization from granodiorites with emergence of a negative Eu anomaly, is usually attributed to crystallization of minerals-concentrators of REE – monocytes and apatite – and to their withdrawal from magma [Miller, Mittlefehdt, 1982]. Granites with a positive Eu anomaly rarely occur in nature, but happen to occur among the Early Precambrian TTG associations, or less commonly in the present-day geodynamic frameworks [Martin, 1999]. With rare exceptions [Kunina, Mints, 1993; Petrova et al., 1999], their formation is also regarded in the context of magma differentiation [Art et al., 1978; Sheppard et al., 2001]. However, most researchers, who consider the REE distribution in rocks, either do not explain the reasons for the emergence of Eu anomaly or, in case of its positive value, relate it to a large amount of plagioclase in rocks and, therefore, to that of Ca-Sr pairs where there is isomorphic substitution of europium for strontium [Taylor, McLennan, 1988]. In our case, however, there is no correlation between the size of a positive Eu anomaly and the strontium content.

Geological nature of the veined granites with a positive Eu anomaly is ambiguously interpreted by scientists. This is to a certain extent related to their frequent occurrence among "grey gneisses" of the Archean TTG series, the genesis of which, in its, turn, is rather disputable. Most western scientists accept that "grey gneisses" were formed by magmatic crystallization and that the veined granites with a positive Eu anomaly are the final products of this process [Sheppard et al., 2001]. Most of the Russian scientists consider that "grey gneisses" are the products of metasomatic transformation of the basite substrate and relate granites with a positive Eu anomaly to the final – microcline – stage of the granitization process [Kunina, Mints, 1993].

There is much evidence indicating that the central parts of dome-shaped structures of the Northern Ladoga region are composed the Archean grey gneisses. However, the intersecting veins therein are interpreted to have formed during brittle deformation in these rocks in the Paleoproterozoic and it may be expected that some of these "grey gneisses" comprising the central part of the domes, with positive Eu anomalies, are earlier-formed. The examples provided herein demonstrate the occurrence of Eu anomalies in plagioclase granites. However, it is also quite common that such anomalies occur also in potassium varieties. Thus, an actual decrease in total REE content in the TTG rock series with an increase in silica content, and the opinion that the granites of these series are formed at the final stage of metasomatic development in the zone of contact with the initial basite substrate may give the impression of residual nature of a positive Eu anomaly, i.e. of the complete final-stage withdrawal of REE and almost unchanged concentrations of Eu [Mints et al., 1996], but Ba supply is obvious in our case so that the complete withdrawal of microelements remains uncertain.

Other important natural formations with a positive Eu anomaly are oil, coal [Balashov, Tsoi, 1989], phosphorites [Baturin et al., 2001], and Archean ferruginous quartzites [Danielson et al., 1992]. High concentration of Eu in these rocks is an indicator of rapid restoration of their formation environment. It has long been argued that europium which is present in barite has a valence of 2 and isomorphically substitutes for barium [Guichard et al., 1979]. The presence of barite has been further suggested as a cause of the occurrence of positive Eu anomaly in bauxite ores which may contain autigenic barite. An abnormal behavior of europium can be attributed to rapid environmental restoration during phosphorus diagenesis [Baturin, 2004].

A direct correlation between the size of Eu anomaly and barium content was noted by the Indian scientists who described Eu-rich Late Proterozoic-Cambrian phosphorite deposits of the Lower Himalayas. The same rocks are also known for an inverse correlation between a positive Eu anomaly and strontium content which indicates Eu entry into barite phase [Mazumdar et al., 1999]. This case is similar to ours in which no direct correlation has been found between the positive Eu anomaly size and strontium and total REE contents, and yet there is a direct correlation between barium concentration and a positive Eu anomaly that may indicate the presence of barium phase (barium mineral itself, for example). The significance of barium marker in the interpretation of the Early Precambrian tectonic environment was first referred to in [Glukhovsky, Moralev, 1997].

Considering that the Eu^{++}/Eu^{+++} ratio value is a function of reduction-oxidation potential of mineral formation environments, the granitoids with positive Eu anomaly can also be thought of as formed in reducing environment. What is the reason of occurrence of such fluids at final stages of metamorphism and granitization?

Most of the granites studied are high-alumina which may relate their formation period to active tectonic events. Thus, the origin of high-alumina granites has long been attributed to partial melting of the crustal rocks during the continental collision [Sheppard et al., 2001; Martin, 1999], though there are also the models of similar-granite formation as a result of partial melting caused by intrusion of hot mantle magmatic masses into the bottom of the Earth's crust, i.e., as a result of underplating processes [Williamson et al., 1992]. The geneses of the studied small granite veins confined to different complexes and, probably, not similar in age are not compatible with any of the above-mentioned models which imply the formation of gigantic batholiths whose constituent granites have typical negative Eu anomalies. In our case, these are small cavity-filling bodies or ptygmatite-like segregations which did not evolve through the stage of magma melting. The presence of a positive Eu anomaly implies the formation of veined granites in reducing conditions, and their high barium content which is typical of deep-seated fluid-saturated formations such as kimberlites and lamproites and post-folding intrusion rocks support this assumption.

Here is a model of geodynamic environment in which the studied rocks may have been formed. The brittle-plastic transition zone in the Earth's crust, to which the formation of the rocks studied is confined, has received growing attention from geologists, geophysicists, and geochemists. This is precisely the area that is now considered by many scientists as an important crustal interface ("barrier zone") which prevents fluids and deep-seated rocks from coming up to the surface [Ivanov, Rusin, 1997]. Extreme conditions, such as crustal extension, hummocking or formation of deep pull-apart structures, cause damage to this barrier so that deep-seated, mostly reduced fluids break through and thus give rise to formation of different veined bodies or blastomylonitic belts. There occurs the withdrawal of most of the ore-forming elements and their subsequent precipitation in the upper-crust levels. A large amount of veins composed of the rocks with a positive Eu anomaly and their small dimensions imply rather specific tectogenetic conditions in this area, caused by its confindness to the transition zone between the Svecofennides and the Karelsky massif and the presence of basement rocks which acted as a fluid trap up to a certain point in time and decomposed under deep-seated fluid load later on. It is precisely these fluids that led to the formation of granites with a positive Eu anomaly, and to withdrawal of most of the microelements ("hydrogen blowing") and their precipitation in the upper crustal section. Note that this fluid trap may decompose more than once and in different structural environments. Thus, the multi-year research conducted in the Northern Ladoga region allowed us to identify similar structural parageneses of three sequential stages of deformations, both inside the protrusions and in surrounding areas. This allows drawing a conclusion on the uniform geomechanical formation conditions of the Svecofennian tectonic structure in the cover and in the rheomorphosed basement and, respectively, considering felsic veins as indicators of certain deformation stages. The presence of single-type veined granitoids with a positive Eu anomaly in the basement and in the cover confirms our structural suggestions about the unified character of the basement-cover system transformations.

The earliest plagiogranite veins, in dome-shaped basement protrusion Havus conjugated with the fold-thrust structures imposed on the initial basite dykes, yielded ages of about 1870 Ma, thus indicating the upper time limit for the first kinematic stage of Svecofennian tectogenesis. Most of the samples from the first-stage veins have a positive

Eu anomaly. The veined bodies which are associated with the second-stage deformation structures (linear folds of NW and sub-meridional strike imposed on thrust sheets) yielded ages of about 1830 Ma (1827.9±4.9; 1828.1±4.9 Ma) both in Sortavala and Ladoga series. The submeridional stripes of massive varieties we found in the gneissized TTG rock bodies yielded the same age of 1828.6±4.3 Ma as an indicative manifestation of palingenetic processes peaked with the Svecofennian deformation events. The NE-striking intense schistosity zones representing chlorite-sericite subfacies (third regional deformation stage), which are imposed on the early kinematic granite bodies (Havus protrusion), yielded zircon shells and single metamict-zircon grains with ages of 1768±6–1755.1±4.3 Ma, probably reflecting the time interval for manifestation of orogenic processes in the region [Morozov et al., 2018].

Evidence has been found that the analyzed REE spectra in the cross-cutting structural-paragenetic markers already mentioned – in granite and pegmatoid bodies of sequential deformation stages – change regularly both in dome-shaped protrusions and their covers (involving primarily a zone of amphibolite facies metamorphism). The veined bodies embedded in structural parageneses of the first and third deformation stages show a consistently positive Eu anomaly whereas similar formations of the intermediate, second stage of tectogenesis display a negative Eu anomaly. Considering the questionable nature of a positive Eu anomaly in the rocks of the Precambrian continental crust and varied causes of its occurrence, the highest importance would be attached to several factors. Its manifestation in partially rheomorphosed substrate of the Archean basement may be due to the presence of "grey-gneiss" protolith which is known to have markedly higher Eu content. The other factor may be that the processes of partial melting during the basement rheomophism also influence on Eu concentration. Finally, the most important and the most appropriate factor may be a temporal succession of redox conditions of the fluid regime which, in its turn, depends on the depth at which the transformations occur and on geodynamic environment. The subsequent thermal heat, rheomorphism of the basement, and granitizing fluid flow which reached its maximum by the middle of the Svecofennian tectogenesis (stage D2) shifted the balance toward the oxidized environment and, therefore, to a marked decrease of concentrations. The third-stage transition from the processes or tectogenesis, with primarily convergent geodynamics, to orogenic events, with an increasing participation of brittle faults draining the lower crust horizons, shifted the balance backward to reducing fluid regime which provided correspondingly higher Eu contents. However, it is quite obvious that Eu "markers" and their concordant changes at different tectogenetic stages may serve as an additional criterion and a proof for joint transformations of the cover and basement complexes under unified and common conditions and environments.

6. CONCLUSIONS

A polymetamorphic complex in the Northern Ladoga region contains abundant acid veined bodies with a positive Eu anomaly. The results obtained testify to an important geochemical aspect of the rare-earth elements in granitoids from the veined bodies, related primarily to somewhat excessive behavior of their-contained Eu anomaly, thus implying a reducing environment that encourages the search for geodynamic causes of extraordinary formation conditions.

Visually and petrographically similar pegmatoid veins may differ largely in terms of microelement content, especially in terms of the presence of the Eu anomaly. The varieties, which have this anomaly, are always high in barium, and there in direct correlation between the size of Eu anomaly and $(La/Yb)_n$, Ca and Sr. This contradicts the prevailing ideas of the occurrence of a positive Eu anomaly exclusively through the substitution of divalent strontium by Eu.

High barium contents are typical of the post-fold intrusions in the region and also of kimberlites and lamproites, i.e., of the complexes genetically related to the deep mantle processes and high fluid saturation so that the acid veined bodies with anomalously high barium contents may be channels for penetration of deep fluid flows. The studied veins, anomalously high in barium, are probably the link between the deep zones and hydrothermal processes where barium mainly accumulates in the form of its major mineral – the barite.

The rise of reduced fluids to the surface and, respectively, the formation of acid veined rocks occurred under certain dynamic conditions in the brittle deformation environment.

Three stages distinguished in geodynamic evolution of the region (beginning of basement crushing and thrusting (D1), development of folded deformations (D2) and post-fold orogenesis (D3)) are characterized by the presence of veined bodies with a positive Eu anomaly at the first and last stages in the evolution of the structure when there was a predominance of brittle deformations and a rise of reduced fluids to the surface. At the second stage, when the crust was dominated by plastic deformations, there occurred a blockage of the flow of fluids and formation of granitoids with low barium contents and a negative Eu anomaly.

7. CONTRIBUTION OF THE AUTHORS / ЗАЯВЛЕННЫЙ ВКЛАД АВТОРОВ

The authors contributed equally to this article.

Все авторы внесли эквивалентный вклад в подготовку публикации.

8. CONFLICT OF INTERESTS / КОНФЛИКТ ИНТЕРЕСОВ

The authors have no conflicts of interest to declare. All authors have read and agreed to the published version of the manuscript.

Авторы заявляют об отсутствии у них конфликта интересов. Все авторы прочитали рукопись и согласны с опубликованной версией.

9. REFERENCES

Art J.G., Barker F., Peterman Z.E., Friedman I., 1978. Geochemistry of Gabbro-Diorite-Tonalite-Trondhjemite Suite of Southwest Finland and Its Implications for the Origin of Tonalitic and Trondhjemitic Magmas. Journal of Petrology 19 (2), 289–316. https://doi.org/10.1093/petrology/19.2.289.

Balashov Yu.A., Tsoi K.S., 1989. A Role of Reducing Environments in Eu^{2+}, Yb^{2+} and Sm^{2+} Accumulation in Oils. Doklady of the USSR Academy of Sciences 309 (5), 1189–1192 (in Russian) [Балашов Ю.А., Цой К.С. Роль окислительно-восстановительных условий в накоплении Eu^{2+}, Yb^{2+}, Sm^{2+} в нефтях // Доклады АН СССР. 1989. Т. 309. № 5. С. 1189–1192].

Baltybaev Sh.K., Glebovitskii V.A., Kozyreva I.V., Konopelko D.L., Levchenkov O.A., Sedova I.S., Shuldiner V.I., 2000. Geology and Petrology of the Svecofennides of the Ladoga Region. Saint Petersburg University Press, Saint Petersburg, 200 p. (in Russian) [Балтыбаев Ш.К., Глебовицкий В.А., Козырева И.В., Конопелько Д.Л., Левченков О.А., Седова И.С., Шульдинер В.И. Геология и петрология свекофеннид Приладожья. СПб.: Изд-во СПбГУ, 2000. 200 с.].

Baltybaev Sh.K., Glebovitskii V.A., Kozyreva I.V., Shul'diner V.I., 1996. The Meyeri Thrust: The Main Element of the Suture at the Boundary between the Karelian Craton and the Svecofennian Belt in the Ladoga Region of the Baltic Shield. Doklady Earth Sciences 348 (4), 581–584 (in Russian) [Балтыбаев Ш.К., Глебовицкий В.А., Козырева И.В., Шульдинер В.И. Мейерский надвиг – главный элемент строения сутуры на границе Карельского кратона и свекофеннского комплекса в Приладожье, Балтийский щит // Доклады АН. 1996. Т. 348. № 3. С. 353–356].

Baltybaev Sh.K., Levchenkov O.A., Levskii L.K., 2009. Svecofennian Belt of the Fennoscandia: Spatiotemporal Correlation of the Early Proterozoic Endogenous Processes. Nauka, Saint Petersburg, 328 p. (in Russian) [Балтыбаев Ш.К., Левченков О.А., Левский Л.К. Свекофеннский пояс Фенноскандии: пространственно-временная корреляция раннепротерозойских эндогенных процессов. СПб.: Наука, 2009. 328 с.].

Baturin G.N., 2004. Phosphate Accumulation in Ocean. Nauka, Moscow, 460 p. (in Russian) [Батурин Г.Н. Фосфатонакопление в океане. М.: Наука, 2004. 460 с.].

Baturin G.N., Lucas J., Prevot-Lucas L., 2001. The Europium Anomaly in Oceanic Phosphorites. Doklady Earth Sciences 379A (6), 701–704.

Beus A.A., 1981. Geochemistry of the Lithosphere. Nauka, Moscow, 335 p. (in Russian) [Беус А.А. Геохимия литосферы. М.: Наука, 1981. 335 с.].

Bowes D.R., Halden N.M., Koistinen T.J., Parc A.F., 1984. Structural Features of Basement and Cover Rocks in the Eastern Svecokarelides, Finland. In: A. Kroner, R. Greiling (Eds), Precambrian Tectonics Illustrated. Schweizerbart Science Publishers, Stuttgart, Germany, p. 147–171.

Danielson A., Moller P., Dulski P., 1992. The Europium Anomales in Banded Iron Formation and the Thermal History of Oceanic Crust. Chemical Geology 97 (1–2), 89–100. https://doi.org/10.1016/0009-2541(92)90137-T.

Erlang A., 1972. Correlation between Potassium and Rubidium Contents in the Earth's Rock. In: Origin and Distribution of the Elements. Mir, Moscow, p. 70–88 (in Russian) [Эрланг А. Связь между содержаниями калия и рубидия в земных породах // Распространенность элементов в земной коре. М.: Мир, 1972. С. 70–88].

Eskola P.E., 1948. The Problem of Mantled Gneiss Domes. Quarterly Journal of the Geological Society 104, 461–476. https://doi.org/10.1144/GSL.JGS.1948.104.01-04.21.

Fadin Ya.Yu., Panova E.G., Oleinikova G.A., Voronin D.O., 2016. Geochemical Features of Black Shales from Narke Deposits (Sweden). Vestnik of Saint Petersburg University. Earth Sciences 7 (2), 27–36 (in Russian) [Фадин Я.Ю., Панова Е.Г., Олейникова Г.А., Воронин Д.О. Геохимические особенности черных сланцев месторождений района Нарке (Швеция) // Вестник СПбГУ. 2016. Т. 7. № 2. С. 27–36]. https://doi.org/10.21638/11701/spbu07.2016.203.

Glebovitskii V.A., Baltybaev Sh.K., Levchenkov O.A., Berezhnaya N.G., Levskii L.K., 2002. Age, Duration, and PT Parameters of the Multistage Metamorphism of Svecofennides of the Ladoga Region, Baultic Shield: Evidence from Thermobarometry and U-Pb Geochronology. Doklady Earth Sciences 385 (5), 483–487.

Glukhovskii M.Z., Moralev V.M., 1997. The Ba Signature of the Ancient Continental Crust: Tectonic Implications. Geotectonics 5, 345–358.

Guichard F., Church T.M., Treuil M., Jaffrezic H., 1979. Rare Earth Elements in Barites: Distribution and Effects on Aqueous Partitioning. Geochimica et Cosmochimica Acta 43 (7), 983–997. https://doi.org/10.1016/0016-7037(79)90088-7.

Ivanov S.N., Rusin A.I., 1997. Continental Rift Metamorphism. Geotectonics 1, 3–15.

Joosua L., Leplanda A., Kreitsmanna T., Üprausd K., Robertse N., Paistea P., Martine A., Kirsimäe K., 2016. Petrography and the REE-Composition of Apatite in the Paleoproterozoic Pilgujärvi Sedimentary Formation, Pechenga

Greenstone Belt, Russia. Geochimica et Cosmochimica Acta 186, 135–153. https://doi.org/10.1016/j.gca.2016.04.043.

Kostitsyn Yu.A., 2000. Accumulation of Rare Elements in Granites. Priroda 1, 21–31 (in Russian) [Костицын Ю.А. Накопление редких элементов в гранитах // Природа. 2000. № 1. С. 21–31].

Kulakovsky A.L., Morozov Yu.A., Smul'skaya A.I., 2015. Tectonic Stress as Additional Thermodynamic Factor of Metamorphism (Northern Ladoga Region). Geophysical Research 16 (1), 44–68 (in Russian) [Кулаковский А.Л., Морозов Ю.А., Смульская А.И. Тектонический стресс как дополнительный термодинамический фактор метаморфизма // Геофизические исследования. 2015. Т. 16. № 1. С. 44–68].

Kunina N.M., Mints M.V., 1993. The Behavior of Rare-Earth Elements during Granitization. Bulletin of Moscow Society of Naturalists. Geological Section 68 (4), 86–94 (in Russian) [Кунина Н.М., Минц М.В. Поведение редкоземельных элементов в процессе гранитизации // Бюллетень МОИП. Отдел Геологический. 1993. Т. 68. № 4. С. 86–94].

Lukanin O.A., Dernov-Pegarev V.F., 2009. Main Factors Determining the Occurrence of the Europium Anomaly in Fluids Formed during the Pressure-Drop-Induced Degassing of Granite Magmas. Scientific Herald of the Earth Sciences Department of RAS 1 (27) (in Russian) [Луканин О.А. Дернов-Пегарев В.Ф. Основные факторы, определяющие появление европиевой аномалии во флюидах, образующихся при дегазации гранитных магм, вызванной снижением давления // Вестник Отделения наук о Земле РАН. 2009. № 1 (27)]. Available from: https://onznews.wdcb.ru/publications/asempg/magm-24.pdf (Last Accessed April 5, 2021).

Makeyev A.B., Skublov S.G., 2016. Y–REE-Rich Zircons of the Timan Region: Geochemistry and Economic Significance. Geochemistry International 54, 788–794. https://doi.org/10.1134/S0016702916080073.

Makrygina V.A., Petrova Z.I., 1996. Geochemistry of Migmatites and Granitoids of Priol'khon'e and Ol'khon Island, Baikal Region. Geochemistry International 34 (7), 574–585.

Martin H., 1999. Adakitic Magmas: Modern Analogues of Archaen Granitoids. Lithos 46 (3), 411–429. https://doi.org/10.1016/S0024-4937(98)00076-0.

Mazumdar A., Banerjee D.M., Schidlovski M., Balaram V., 1999. Rare-Earth Elements and Stable Isotope Geochemistry of Early Cambrian Chert-Phosphorite Assemblages from the Lower Tal Formation of the Krol Belt Lesser Himalaya, India. Chemical Geology 156 (1–4), 175–297. https://doi.org/10.1016/S0009-2541(98)00187-9.

Mehnert K.R., 1971. Migmatites and the Origin of Granitic Rocks. Mir, Moscow, 328 p. (in Russian) [Менерт К. Мигматиты и происхождение гранитов. М.: Мир, 1971. 328 с.].

Miller C.F., Mittlefehdt D.W., 1982. Depletion of Light Rare-Earth Elements in Felsic Magmas. Geology 10 (3), 129–133. https://doi.org/10.1130/0091-7613(1982)10<129:DOLREI>2.0.CO;2.

Mints M.V., Glaznev V.N., Konilov A.N., Kunina N.M., Nikitichev A.P., Raevskii A.B., Sedykh Yu.N., Stupak V.M., Fonarev V.I., 1996. The Early Precambrian of the Northeastern Baltic Shield: Paleogeodynamics, Structure and Evolution of the Continental Crust. Proceedings GIN RAS. Iss. 503. Naychny Mir, Moscow, 278 p. (in Russian) [Минц М.В., Глазнев В.Н., Конилов А.Н., Кунина Н.М., Никитичев А.П., Раевский А.Б., Седых Ю.Н., Ступак В.М., Фонарев В.И. Ранний докембрий северо-востока Балтийского щита: палеогеодинамика, строение и эволюция континентальной коры// Труды ГИН РАН. М.: Научный мир, 1996. Вып. 503. 278 с.].

Morozov Yu.A., 1999. The Role of Transpression in the Structural Evolution of the Svecokarelides in the Baltic Shield. Geotectonics 33 (4), 302–313.

Morozov Yu.A., 2002. Structure-Formation Function of Transpression and Transtension. Geotectonics 36 (6), 431–450.

Morozov Yu.A., Bayanova T.B., Matveev M.A., Kulakovskiy A.L., Smulskaya A.I., 2018. Age-Associated Features of Early and Late Svecofennian Tectogenetic Events in the Southeast of the Baltic Shield (Northern Domain of the Ladoga Region). In: Problems of Tectonics and Geodynamics of the Earth's Crust and Mantle. Proceedings of the L Tectonic Meeting (January 30 – February 3, 2018). Vol. 2. GEOS, Moscow, p. 34–39 (in Russian) [Морозов Ю.А., Баянова Т.Б., Матвеев М.А., Кулаковский А.Л., Смульская А.И. Возрастные метки ранне- и позднетектонических событий свекофеннского тектогенеза на ЮВ Балтийского щита (северный домен Приладожья) // Проблемы тектоники и геодинамики земной коры и мантии: Материалы L Тектонического совещания (30 января – 3 февраля 2018 г.). М.: ГЕОС, 2018. Т. 2. С. 34–39].

Morozov Yu.A., Gaft D.E., 1985. On the Nature of Granite-Gneiss Domes in the Northern Ladoga Region. In: V.V. Ez (Ed.), Structure and Petrology of the Precambrian Complexes. Publishing House of the Institute of the Physics of the Earth of the USSR Academy of Science, Moscow, p. 3–120 (in Russian) [Морозов Ю.А., Гафт Д.Е. О природе гранитогнейсовых куполов Северного Приладожья // Структура и петрология докембрийских комплексов / Ред. В.В. Эз. М.: ИФЗ АН СССР, 1985. С. 3–120].

Morozov Yu.A., Somin M.L., 1997. Structural and Thermal Consequences of the Basement-Cover Interaction in Mobile Belts. In: A.V. Lukyanov (Ed.), Structural Parageneses and Their Ensembles. GEOS, Moscow, p. 122–124 (in Russian) [Морозов Ю.А., Сомин М.Л. Структурные и термические следствия взаимодействия чехла и фундамента в подвижных поясах // Структурные парагенезы и их ансамбли / Ред. А.В. Лукьянов. М.: ГЕОС, 1997. С. 122–124].

Morozov Yu.A., Somin M.L., Travin V.V., 2000. The Behavior of Granitoid Basement Involved in the Formation of the Svecokarelian Foldbelt, Northern Ladoga Region. Doklady Earth Sciences 370 (1), 58–62.

Morozov Yu.A., Yudin D.S., Travin A.V., Matveev M.A., Kulakovskiy A.L., Smulskaya A.I., 2020. The First Discovery of Pseudotachylytes in the Paleoproterozoic Ladoga Zonal Metamorphosed Complex of Fennoscandia and Their $^{40}Ar/^{39}Ar$ Dating. Doklady Earth Sciences 493, 485–489. https://doi.org/10.1134/S1028334X20070119.

Myskova T.A., Mil'kevich R.I., L'vov P.A., 2012. U-Pb Geochronology of Zircons from Metasediments of the Ladoga Group (North Ladoga Region, Baltic Shield). Stratigraphy and Geological Correlation 20, 166–178. https://doi.org/10.1134/S0869593812020062.

Nagaitsev Yu.V., 1974. Petrology of the Rocks from the Ladoga and Belomorye Metamorphic Complexes. Publishing House of Leningrad State University, Leningrad, 160 p. (in Russian) [Нагайцев Ю.В. Петрология метаморфических пород ладожского и беломорского комплексов. Л.: Изд-во ЛГУ, 1974. 160 с.].

Nironen M., 1997. The Svekofennian Orogen: A Tectonic Model. Precambrian Research 86 (1–2), 21–44. https://doi.org/10.1016/S0301-9268(97)00039-9.

Norman M.D., Leeman W.P., Mertman S.A., 1992. Granites and Rhyolites from Northwestern U.S.A.: Temporal Variation in Magmatic Processes and Relations to Tectonic Setting. Transactions of the Royal Society of Edinburgh: Earth Sciences 83 (1–2), 71–81. https://doi.org/10.1017/S0263593300007768.

Okina O., Lyapunov S., Avdosyeva M., Ermolaev B., Golubchikov V., Gorbunov A., Sheshukov V., 2016. An Investigation of the Reliability of HF Acid Mixtures in the Bomb Digestion of Silicate Rocks for the Determination of Trace Elements by ICP-MS. Geostandards and Geoanalytical Research 40 (4), 583–597. https://doi.org/10.1111/ggr.12124.

Park A.F., Bowes D.R., 1983. Basement-Cover Relationships during Polyphase Deformation in the Svecokarelides of the Kaavi District, Eastern Finland. Transactions of the Royal Society of Edinburgh: Earth Sciences 74 (2), 95–118. https://doi.org/10.1017/S0263593300010191.

Park A.F., Bowes D.R., Halden N.M., Koistinen T.J., 1984. Tectonic Evolution at an Early Proterozoic Continental Margin: The Svecokarelides of Eastern Finland. Journal of Geodynamics 1 (3–5), 359–386. https://doi.org/10.1016/0264-3707(84)90016-4.

Petrova Z.I., Makrygina V.A., Bobrov V.A., 1999. Rare-Earth Elements as Indicators of the Geodynamic Evolution in the Continental Block of the Ol'khon Island and Adjacent Areas, Western Baikal Region. Geochemistry International 37 (12), 1158–1168.

Rudnick R.L., 1992. Restites, Eu Anomalies and Lower Continental Crust. Geochimica et Cosmochimica Acta 56 (3), 963–970. https://doi.org/10.1016/0016-7037(92)90040-P.

Salop L.I., 1979. The Gneiss-Granulite Complex as a Basement of the Karelides in the Ladoga Region and the Svecofennides in the South of Finland. Bulletin of Moscow Society of Naturalists. Geological Section 54 (5), 3–17 (in Russian) [Салоп Л.И. Гнейсо-гранулитовый комплекс – фундамент карелид в Приладожье и свекофеннид на юге Финляндии // Бюллетень МОИП. Отдел Геологический. 1979. Т. 54. № 5. С. 3–17].

Sedova I.S., Samorukova L.M., Glebovitsky V.A., Krylov D.P., 2004. Geochemistry of Granitoids of the Svecofennian Tectonometamorphic Cycle in the Northern Ladoga Region. Petrology 12 (4), 348–366.

Sharov N.V. (Ed.), 2020. Proterozoic Ladoga Structure (Geology, Deep Structure and Minerageny Genesis), KarRC RAS, Petrozavodsk, 435 p. (in Russian) [Ладожская протерозойская структура (геология, глубинное строение и минерагения) / Ред. Н.В. Шаров. Петрозаводск: Изд-во КарНЦ РАН, 2020. 435 с.].

Shcherbakova T.F., 1988. The Amphibolites of the Belomorye Complex and Their Granitization. Nauka, Moscow, 149 p. (in Russian) [Щербакова Т.Ф. Амфиболиты Беломорского комплекса и их гранитизация. М.: Наука, 1988. 149 с.].

Sheppard S., Griffin T.J., Tyler I.M., Page R.W., 2001. High- and Low-K Granites and Adakites at a Paleoproterozoic Plate Boundary in Nortwern Australia. Journal of the Geological Society 158 (3), 547–560. https://doi.org/10.1144/jgs.158.3.547.

Shuldiner V.I., Kozyreva I.V., Baltybaev Sh.K., Povarkova A.V., Khrestenkov S.A., 1995. Plutonic and Metamorphic Evolution of the Western Ladoga Region: a New Model. Regional Geology and Metallogeny 4, 52–62 (in Russian) [Шульдинер В.И., Козырева И.В., Балтыбаев Ш.К., Поваркова А.В., Хрестенков С.А. Плутоно-метаморфическая эволюция Западного Приладожья: новая модель // Региональная геология и металлогения. 1995. № 4. С. 52–62].

Sudovikov N.G., Glebovitskii V.A., Sergeev A.S., Petrov V.P., Kharitonov A.L., 1970. Geological Development of the Depth Zones in the Mobile Belts (Northern Ladoga Region). Nauka, Leningrad, 227 p. (in Russian) [Судовиков Н.Г., Глебовицкий В.А., Сергеев А.С., Петров В.П., Харитонов А.Л. Геологическое развитие глубинных зон подвижных поясов (Северное Приладожье). Л.: Наука, 1970. 227 с.].

Sylvester P.J., 1998. Post-Collisional Strongly Peraluminous Granites. Lithos 45 (1–4), 29–44. https://doi.org/10.1016/S0024-4937(98)00024-3.

Taylor S.R., McLennan S.M., 1988. Continental Crust: Its Composition and Evolution. Mir, Moscow, 384 p. (in Russian) [Тейлор С.Р., Мак-Леннан С.М. Континентальная кора: ее состав и эволюция. М.: Мир, 1988. 384 с.].

Terekhov E.N., Baluev A.S., 2011. Post-Folding Magmatism (1.85–1.7 Ga) in the Eastern Part of the Baltic Shield: Correlation of Its Structural Position and Evolution of Surrounding Complexes. Stratigraphy and Geological Correlation 19, 600–617. https://doi.org/10.1134/S0869593811060074.

Terekhov E.N., Levitsky V.I., 1993. The Lapland Granulite Belt: Rare-Earth Elements and Problems of Petrogenesis. Proceedings of Higher Educational Establishments. Geology and Exploration 5, 3–17 (in Russian) [Терехов Е.Н., Левицкий В.И. Гранулиты Лапландского пояса: редкоземельные элементы и проблемы петрогенезиса // Известия вузов. Геология и разведка. 1993. № 5. С. 3–17].

Terekhov E.N., Shcherbakova T.F., 2006. Genesis of Positive Eu Anomalies in Acid Rocks from the Eastern Baltic Shield. Geochemistry International 44, 439–455. https://doi.org/10.1134/S0016702906050028.

Terekhov E.N., Shcherbakova T.F., Konilov A.N., 2016. Olivine-Bearing Rocks of the Lapland Granulite Belt (Baltic Shield). Geochemistry International 54, 964–978. https://doi.org/10.1134/S001670291609010X.

Velikoslavinskii D.A., 1972. Comparative Characteristics of the Moderate- and Low-Pressure Regional Metamorphism. Nauka, Leningrad, 190 p. (in Russian) [Великославинский Д.А. Сравнительная характеристика регионального метаморфизма умеренных и низких давлений. Л.: Наука, 1972. 190 с.].

Watson J., Dunning F.W., 1979. Basement-Cover Relations in the British Caledonides. In: A.L. Harris, C.H. Holland, B.E. Leake (Eds), The Caledonides of the British Isles – Reviewed. Geological Society of London, p. 67–91.

Williamson B.J., Downes H., Trirlwall F.M., 1992. The Relationship between Crustal Magmatic Underplating and Granite Genesis: An Example from the Velay Granite Complex, Massif Central, France. In: The Origin of Granites and Related Rocks. Transactions of the Royal Society of Edinburgh: Earth Sciences 83 (1–2), 235–245. https://doi.org/10.1017/S0263593300007926.

APPENDIX 1 / ПРИЛОЖЕНИЕ 1

Table 1.1. Representative analyses of veined granitoids with a positive Eu anomaly from different stratigraphic complexes in the Northern Ladoga region

Таблица 1.1. Представительные анализы жильных гранитоидов с положительной Eu-аномалией из различных стратиграфических комплексов Северного Приладожья

Component	Sample						
	ЛВ-1742	ЛВ-1946/4	ЛВ-1875/2	ЛВ-1948/1	ЛВ-1951	ЛВ-1703/1	ЛВ-1703/1
	1	2	3	4	5	6	7
SiO_2	75.77	67.45	64.78	75.59	71.88	67.16	75.40
TiO_2	<0.01	0.15	0.95	<0.01	0.02	0.27	0.12
Al_2O_3	14.53	18.27	16.09	14.67	16.86	18.96	12.87
Fe_2O_3	0.19	0.32	4.57	0.08	0.18	1.74	0.90
FeO	0.17	1.95	–	0.81	0.78	–	–
MnO	<0.01	0.06	0.05	0.02	0.02	0.02	0.01
MgO	0.10	0.62	1.64	0.07	0.15	0.60	0.39
CaO	1.25	4.71	3.25	2.31	2.13	2.76	0.72
K_2O	2.67	1.05	2.61	0.63	0.84	1.69	5.61
Na_2O	4.30	4.50	4.36	5.42	6.22	5.87	2.94
P_2O_5	0.04	0.06	0.38	<0.01	0.04	0.11	0.02
LOI	0.78	0.48	0.96	0.26	0.68	0.66	0.55
Total	99.80	99.63	99.63	99.86	99.78	99.84	99.53
Li	7.3	21	21	7.0	12.3	15	7.5
Be	1.92	1.57	2.0	13.9	11.8	2.1	0.60
Sc	0.84	2.5	6.7	0.52	1.00	2.7	0.72
V	0.74	18	57	3.1	4.2	21	9.6
Cr	21	55	57	61	69	<8	<8
Co	0.58	4.6	9.5	1.08	1.33	2.3	2.4
Ni	5.3	9.3	9.5	6.9	2.7	2.2	3.4
Cu	16	28	30	21	32	21	41
Ga	9.3	18.4	22	26	25	22	14
Rb	44	40	62	25	34	39	96
Sr	246	608	900	91	279	460	457
Y	10.4	6.0	11	10.7	11.6	4.4	0.9
Zr	8.4	79	315	10.6	19.1	74	44
Nb	0.85	3.5	16	3.1	5.3	8.5	1.6
Mo	2.1	4.0	4.4	6.5	6.5	0.91	0.89
Sn	<0.7	0.7	0.9	<0.7	0.8	0.28	0.3
Sb	0.08	0.28	–	0.23	0.34	–	–
Cs	0.54	1.66	0.63	1.92	1.39	0.72	0.40
Ba	1151	348	1759	49	447	692	4482
La	3.8	12.1	54	3.2	3.2	22	12
Ce	5.9	21	104	5.7	6.4	40	22
Pr	0.69	2.5	11	0.57	0.81	4.1	2.1
Nd	2.4	8.5	40	1.94	3.5	14	6.5
Sm	0.55	1.38	6.0	0.62	1.16	2.1	1.1
Eu	1.00	0.71	2.1	0.31	0.50	0.95	1.5
Gd	0.79	1.15	4.0	0.75	1.62	1.5	0.49
Tb	0.17	0.16	0.46	0.16	0.33	0.19	0.047

Table 1.1. (continued)
Таблица 1.1. (продолжение)

Component	Sample						
	ЛВ-1742	ЛВ-1946/4	ЛВ-1875/2	ЛВ-1948/1	ЛВ-1951	ЛВ-1703/1	ЛВ-1703/1
	1	2	3	4	5	6	7
Dy	1.32	0.97	2.4	1.22	2.2	0.90	0.22
Ho	0.32	0.20	0.42	0.32	0.43	0.14	0.036
Er	1.06	0.56	1.1	1.19	1.17	0.33	0.097
Tm	0.17	0.08	0.14	0.23	0.18	0.042	0.016
Yb	1.10	0.55	0.9	1.77	1.17	0.24	0.13
Lu	0.16	0.09	0.14	0.30	0.16	0.038	0.031
Hf	0.31	1.76	6.7	0.52	0.89	1.6	1.5
W	0.23	0.62	0.14	0.47	0.52	0.22	0.04
Tl	0.21	0.16	0.34	0.14	0.24	0.23	0.46
Pb	40.92	17.01	10	29.72	66.64	13	28
Th	0.67	1.65	4.1	8.2	13.9	10.1	4.3
U	0.53	0.87	0.76	7.6	72	0.31	0.36
Ta	0.11	0.33	–	–	–	–	–
(La/Yb)n	2.3	14.8	40	1.2	1.8	61	61
Eu/Eu*	4.8	1.7	1.2	1.4	1.1	1.6	5.4

Note. 1, 2 and 6 – values determined within the rocks of the Ladoga series; 3, 7 – within the rocks of the Sortavala series; 4, 5 – within the basement rocks.
Примечание. 1, 2 и 6 – в породах ладожской серии; 3, 7 – в породах сортавальской серии; 4, 5 – в пределах пород фундамента.

Table 1.2. Data of comparison between the veined granitoids with a positive Eu anomaly and the host rocks
Таблица 1.2. Сравнительные данные жильных гранитоидов с положительной Eu-аномалией и вмещающих пород

Component	П-97/2	П-97/3	П-99/1	П-99/2	П-915/2	П-915/1	П-922/2	П-922/1	П-926/1	П-926/2	П-927/2	П-927/3
	granulite	vein	diorite	vein	schist	vein	amphib.	vein	amphib.	vein	schist	vein
SiO_2	45.17	68.06	61.91	72.29	58.04	72.26	48.31	71.49	47.07	75.46	58.91	70.68
TiO_2	1.89	0.26	0.47	0.02	1.02	0.05	1.38	0.08	2.05	0.05	0.86	0.14
Al_2O_3	14.62	14.15	16.76	15.00	16.91	15.69	12.95	15.73	11.69	14.39	18.06	16.72
Fe_2O_3	3.98	0.82	1.64	0.42	2.74	0.87	5.47	0.42	8.09	0.43	3.08	0.50
FeO	14.08	1.69	2.84	0.96	6.04	0.35	9.97	1.25	11.31	0.76	4.50	1.38
MnO	0.24	0.03	0.12	0.01	0.11	0.01	0.23	0.03	0.24	0.02	0.10	0.05
MgO	5.52	0.99	2.01	0.19	4.19	0.28	6.16	0.45	5.71	0.21	2.74	0.33
CaO	10.18	1.03	4.94	1.11	1.35	0.68	9.64	1.85	8.45	1.76	1.23	2.87
Na_2O	1.92	2.29	4.89	4.22	2.95	3.29	2.82	4.93	2.27	5.21	2.72	4.81
K_2O	0.27	9.19	2.32	5.08	3.84	5.57	0.77	2.85	0.82	1.47	5.13	1.44
P_2O_5	0.20	0.21	0.24	0.00	0.08	0.07	0.17	0.04	0.19	0.01	0.11	0.03
LOI	1.88	0.93	1.62	0.34	2.69	0.68	1.87	0.57	1.75	0.10	2.34	0.67
Total	99.96	99.66	99.76	99.63	99.94	99.79	99.73	99.69	99.64	99.85	99.76	99.62
Li	13.0	16.7	16.6	4.4	74	19.5	23	25	16.1	5.1	49	13.4
Be	0.76	0.41	2.4	4.4	2.1	1.70	0.71	5.9	1.40	6.0	3.7	2.9
Sc	49	5.4	16.5	0.33	26	3.8	47	1.89	45	0.99	19.7	1.76
V	453	31	71	7.9	174	1.96	311	10.0	470	4.5	130	10.6
Cr	79	67	70	59	247	49	71	59	89	32	102	40
Co	62	3.0	12.2	1.42	31	0.95	54	3.0	52	1.36	24	2.7
Ni	71	10.5	19.9	7.4	111	6.3	65	12.9	55	5.8	61	7.9

Table 1.2. (continued)
Таблица 1.2. (продолжение)

Component	П-97/2	П-97/3	П-99/1	П-99/2	П-915/2	П-915/1	П-922/2	П-922/1	П-926/1	П-926/2	П-927/2	П-927/3
	granulite	vein	diorite	vein	schist	vein	amphib.	vein	amphib.	vein	schist	vein
Cu	131	11.9	9.4	8.6	90	9.0	92	13.0	104	10.7	75	19.8
Ga	21	15.5	25	17.6	25	13.3	16.8	20	22	24	27	18.0
Rb	1.33	162	73	72	189	93	10.6	80	36	60	194	45
Sr	227	317	611	366	378	192	179	320	150	106	176	774
Y	27	12.6	25	1.40	29	12.3	25	2.4	38	5.9	24	10.8
Zr	98	27	104	53	163	17.8	102	43	137	36	209	132
Nb	8.5	2.5	4.9	0.66	12.7	3.6	12.2	8.8	8.1	3.6	14.9	10.8
Mo	1.68	5.6	3.1	4.6	3.5	5.2	1.82	7.8	1.25	4.6	1.99	4.2
Sn	0.64	0.80	3.0	0.64	2.6	1.76	0.98	1.58	1.27	0.55	2.7	0.88
Sb	0.082	0.101	0.073	0.087	0.044	0.060	0.068	0.12	0.091	0.095	0.34	0.27
Cs	0.042	0.83	0.67	0.23	13.9	1.57	0.12	1.82	0.59	1.01	8.0	1.42
Ba	37	2645	431	1812	542	1148	185	970	95	215	797	790
La	6.3	19.1	21	4.6	42	3.2	8.3	3.9	6.8	2.3	34	15.3
Ce	16.5	35	54	7.4	82	6.4	21	6.7	18.9	4.6	76	28
Pr	2.5	4.4	8.0	0.81	10.0	0.76	2.7	0.70	3.0	0.58	8.8	3.2
Nd	12.5	17.8	34	3.0	37	2.8	12.5	2.5	14.9	2.3	33	11.8
Sm	3.7	3.9	7.3	0.63	6.7	0.81	3.4	0.63	4.4	0.55	6.5	2.1
Eu	1.37	1.70	0.84	0.42	1.44	0.62	1.07	0.49	1.39	0.34	1.23	0.75
Gd	4.7	3.3	5.7	0.46	6.0	0.95	3.9	0.46	5.7	0.60	5.3	1.75
Tb	0.78	0.43	0.79	0.050	0.88	0.21	0.67	0.076	1.01	0.11	0.77	0.28
Dy	5.0	2.4	4.6	0.27	5.3	1.73	4.4	0.41	6.3	0.76	4.4	1.58
Ho	1.04	0.44	0.89	0.048	1.07	0.40	0.94	0.078	1.29	0.17	0.94	0.32
Er	3.0	1.18	2.5	0.13	3.1	1.29	2.7	0.20	3.7	0.60	2.5	0.92
Tm	0.43	0.16	0.34	0.02	0.44	0.22	0.40	0.028	0.57	0.11	0.36	0.14
Yb	2.8	0.94	2.1	0.15	2.8	1.57	2.7	0.17	3.7	0.74	2.5	0.98
Lu	0.42	0.14	0.29	0.03	0.44	0.23	0.43	0.026	0.57	0.11	0.39	0.16
Hf	2.3	0.62	2.3	1.91	4.1	0.61	2.3	1.18	3.4	1.38	4.9	3.3
W	0.10	0.21	0.17	0.25	0.44	2.0	0.18	0.33	0.14	0.15	1.91	0.37
Tl	0.022	1.53	0.45	0.39	1.21	0.40	0.075	0.41	0.30	0.33	0.90	0.17
Pb	1.26	27	11.0	12.2	24	26	4.1	14.3	8.0	24	18.1	20
Th	0.14	1.72	0.34	1.14	12.4	1.48	0.71	0.62	0.51	9.4	12.2	2.2
U	0.073	0.81	0.24	0.47	3.5	0.84	0.20	0.55	0.45	8.3	3.1	1.69
(La/Yb)N	1.5	13.7	6.7	21	10	1.4	2.1	15.6	1.2	2.1	9.4	10.2
Eu/Eu*	1	1.4	0.39	2.25	0.19	2.16	0.9	2.67	0.84	1.9	0.78	1.2

Table 1.3. Veined granites with a negative Eu anomaly and host rocks
Таблица 1.3. Жильные граниты с отрицательной Eu-аномалией и вмещающие породы

Component	917/1	917/4	918/1	918/2	П-920/1	П-920/2	921/1	921/2	ЛВ-1950	ЛВ-1948/2	ЛВ-1851
	amphib.	vein	amphib.	vein	schist	vein	granite	vein	vein	vein	vein
SiO_2	46.24	74.71	46.45	74.85	62.04	82.96	71.33	73.80	76.07	73.92	70.21
TiO_2	0.48	<0.01	0.90	<0.01	0.74	0.28	0.38	<0.01	0.01	0.05	0.43
Al_2O_3	24.60	14.20	14.46	14.10	16.71	8.06	14.32	14.23	13.31	13.81	16.03
Fe_2O_3	0.22	<0.01	2.66	<0.01	2.77	0.74	<0.01	0.23	0.36	0.03	3.12
FeO	4.87	1.35	10.79	2.00	4.03	1.96	2.64	0.71	0.84	1.21	0.24
MnO	0.14	<0.01	0.24	<0.01	0.06	0.03	0.05	<0.01	0.04	0.02	0.05
MgO	3.10	0.11	7.77	0.15	2.48	0.83	0.69	0.14	0.12	0.17	0.55
CaO	15.50	0.99	12.64	1.13	1.08	1.39	1.76	0.87	0.90	0.73	1.69
Na_2O	2.47	4.17	1.77	4.33	1.77	1.85	3.57	3.67	3.68	5.85	1.31
K_2O	0.78	4.44	0.36	3.71	4.23	0.95	4.38	6.23	4.29	3.71	5.66
P_2O_5	0.04	<0.01	0.06	<0.01	0.15	0.04	0.11	0.06	0.01	0.09	0.11
LOI	1.18	0.14	0.56	0.22	3.67	0.54	0.41	0.18	0.2	0.18	0.72
Total	99.62	100.4	99.66	99.87	99.73	99.62	98.75	99.67	99.83	99.76	99.87
Li	51	4.9	17.8	16.7	48	12.2	73	6.7	9.3	6.7	44
Be	0.17	1.52	0.09	4.9	3.3	2.5	2.0	4.6	6.9	4.8	6.0
Sc	14.6	0.63	23	0.70	17.8	5.8	4.1	0.44	2.3	1.45	6.0
V	146	0.82	319	1.72	107	31	23	1.75	1.89	4.5	28
Cr	76	48	202	79	118	102	49	32	87	76	54
Co	16.8	0.77	55	1.17	18.3	5.4	4.0	0.72	1.03	1.34	4.5
Ni	40	5.7	158	9.1	46	22	6.2	<5	6.4	7.2	4.2
Cu	17.9	10.7	74	14.9	46	21	8.8	16.3	31	20	13
Ga	15.9	15.6	16.8	13.6	24	9.5	19.0	11.8	18.1	19.8	28
Rb	14.7	111	19.7	138	179	52	89	120	233	242	137
Sr	174	32	138	32	97	125	345	166	16.2	59	168
Y	7.6	3.0	15.4	3.6	32	15.1	11.2	4.1	21	15.6	20
Zr	26	47	41	33	224	157	173	87	22	16.9	209
Nb	1.70	10.4	2.0	8.8	13.4	5.1	16.6	3.6	7.1	13.2	22
Mo	0.72	4.2	0.97	5.7	4.6	13.3	4.3	2.5	7.1	10.0	8.5
Sn	0.71	2.2	0.67	2.6	3.0	0.89	3.2	2.5	3.8	1.3	2.1
Sb	1.71	0.10	0.07	0.26	0.050	0.14	0.13	0.21	0.24	0.20	–
Cs	1.93	0.32	4.4	9.3	6.1	1.88	3.2	3.4	12.8	6.0	3.5
Ba	447	36	42	39	572	117	1314	571	42	324	315
La	1.23	4.4	1.82	8.7	48	35	35	13.9	5.4	3.7	36
Ce	2.7	8.7	4.9	15.9	94	69	62	23	10.2	8.7	64
Pr	0.49	0.78	0.85	1.58	11.1	7.5	6.5	2.3	1.16	1.09	6.7
Nd	2.5	3.2	4.6	6.1	40	27	24	7.1	4.0	4.8	24
Sm	0.85	0.93	1.64	1.40	7.2	4.3	4.1	1.49	1.32	1.78	4.2
Eu	0.44	0.18	0.60	0.24	1.28	1.13	1.07	0.44	0.11	0.25	0.53
Gd	1.20	0.69	2.4	1.20	6.1	3.5	3.45	1.05	1.77	2.2	3.2
Tb	0.21	0.10	0.44	0.15	0.90	0.54	0.42	0.15	0.40	0.40	0.49
Dy	1.33	0.55	3.0	0.71	5.7	2.7	2.1	0.78	3.1	2.6	3.0
Ho	0.30	0.12	0.65	0.13	1.13	0.52	0.36	0.14	0.71	0.53	0.58
Er	0.80	0.32	1.80	0.33	3.3	1.39	0.98	0.41	2.3	1.61	1.7
Tm	0.12	0.053	0.27	0.050	0.49	0.20	0.15	0.06	0.39	0.27	0.29
Yb	0.92	0.38	2.1	0.42	3.2	1.29	0.95	0.48	2.7	1.73	2.0
Lu	0.12	0.054	0.26	0.056	0.49	0.19	0.16	0.07	0.39	0.24	0.30
Hf	0.69	2.2	1.13	1.75	5.5	3.8	4.2	3.6	1.12	0.88	4.9

Table 1.3. (continued)

Таблица 1.3. (продолжение)

Component	917/1	917/4	918/1	918/2	П-920/1	П-920/2	921/1	921/2	ЛВ-1950	ЛВ-1948/2	ЛВ-1851
	amphib.	vein	amphib.	vein	schist	vein	granite	vein	vein	vein	vein
W	0.22	0.095	0.055	0.28	1.99	0.62	0.21	0.18	0.67	0.35	0.48
Tl	0.14	0.65	0.091	0.94	0.92	0.24	0.68	0.65	1.36	1.38	0.76
Pb	3.5	48	1.08	36	24	21	19.7	21	36.41	35.14	18
Th	0.41	6.7	0.064	11.3	12.9	6.2	5.8	2.4	9.6	8.4	12
U	0.28	1.75	0.082	2.6	4.4	1.77	2.1	4.0	2.6	5.1	3.1
(La/Yb)N	0.88	7.6	0.58	14	9.8	18	25	19	1.4	1.4	12
Eu/Eu*	1.4	0.6	0.9	0.6	0.59	0.88	0.8	0.95	0.2	0.4	0.42

Table 1.4. Chemical composition of the dome-shaped basement protrusions in the Northern Ladoga region and products of their transformations

Таблица 1.4. Химический состав пород куполовидных выступов фундамента Северного Приладожья и продуктов их преобразований

Component	913/1	914/2	916/1	916/2	916/3	916/4
	1	2	3	5	6	4
SiO_2	74.21	78.77	67.65	72.08	74.88	76.35
TiO_2	0.09	0.10	0.45	0.09	<0.01	<0.01
Al_2O_3	13.05	11.08	15.36	15.50	14.14	13.48
Fe_2O_3	0.14	0.09	0.05	0.06	<0.01	<0.01
FeO	0.60	2.14	3.69	1.42	1.82	1.21
MnO	<0.01	<0.01	0.09	<0.01	0.10	<0.01
MgO	0.17	1.45	1.47	0.22	0.11	0.11
CaO	0.49	2.30	2.75	1.44	0.71	0.69
Na_2O	2.51	3.28	4.06	4.87	4.04	4.06
K_2O	8.27	0.80	1.58	3.29	4.39	4.05
P_2O_5	0.11	0.04	0.12	<0.01	<0.01	<0.01
LOI	0.20	<0.1	2.23	0.72	0.14	0.18
Total	99.67	99.87	99.69	99.89	99.87	99.95
Li	3.0	19.6	156	39	28	33
Be	0.26	2.2	3.9	3.4	3.1	1.71
Sc	0.72	2.4	10.7	1.34	1.55	0.13
V	0.50	34	64	4.4	1.40	1.16
Cr	113	55	52	76	95	38
Co	1.13	5.1	11.5	1.78	0.98	0.73
Ni	36	12.5	16.4	<5	7.4	5.1
Cu	14.5	14.9	11.5	22	39	7.6
Ga	12.1	12.3	24	20	16.8	12.4
Rb	112	41	144	104	163	115
Sr	105	184	175	128	31	116
Y	4.5	4.3	14.3	2.9	17.7	0.65
Zr	52	81	94	79	85	18.9
Nb	3.0	2.6	6.3	14.9	1.89	1.13
Mo	3.3	4.1	4.2	9.0	11.1	2.2
Sn	0.34	0.82	2.7	4.0	1.85	1.13
Sb	0.06	0.15	0.11	0.12	0.17	0.07
Cs	0.39	1.22	5.6	1.80	6.2	1.15

Table 1.4. (continued)
Таблица 1.4. (продолжение)

Component	913/1	914/2	916/1	916/2	916/3	916/4
	1	2	3	5	6	4
Ba	244	87	98	327	51	421
La	7.8	11.9	14.4	11.4	11.6	1.62
Ce	15.6	20	33	16.9	23	2.9
Pr	1.83	2.1	3.5	2.0	2.5	0.24
Nd	6.9	7.6	12.6	6.4	11.6	0.94
Sm	1.42	1.34	2.8	1.21	3.3	0.20
Eu	0.30	0.34	0.73	0.38	0.17	0.19
Gd	1.22	1.18	2.3	0.76	3.1	0.16
Tb	0.17	0.15	0.35	0.089	0.56	0.014
Dy	0.91	0.77	1.99	0.50	3.2	0.07
Ho	0.16	0.14	0.40	0.090	0.67	<0.015
Er	0.38	0.37	1.13	0.24	2.1	0.04
Tm	0.049	0.053	0.16	0.032	0.33	<0.004
Yb	0.28	0.45	1.06	0.24	2.2	0.05
Lu	0.040	0.054	0.15	0.032	0.31	0.008
Hf	1.59	2.5	2.5	2.3	5.2	0.51
W	0.18	0.17	0.14	0.16	0.17	0.082
Tl	0.57	0.20	1.15	0.72	1.20	0.84
Pb	48	5.8	9.4	25	61	19.6
Th	3.4	7.0	5.7	12.4	22.97	3.1
U	2.1	1.11	3.9	2.1	7.2	1.37
Eu/Eu*	0.7	0.8	0.86	1.25	0.2	3
(La/Yb)n	18	18	9.2	32	3.5	25